



New insights into the phylogeny of Stephanidae (Hymenoptera: Apocrita), with a revision of the fossil species

Si-Xun Ge¹, Zhuo-Heng Jiang², Li-Li Ren¹, Cornelis van Achterberg³, Jiang-Li Tan³

¹ College of Forestry, Beijing Forestry University, Beijing 100083, China

² School of Science, Westlake University, Hangzhou, China

³ Shaanxi Key Laboratory for Animal Conservation / Key Laboratory of Resource Biology and Biotechnology in Western China, College of Life Sciences, Northwest University, 229 North Taibai Road, Xi'an, Shaanxi 710069, China

<https://zoobank.org/50EE94AA-D90A-43E1-B54E-4FADE22F4668>

Corresponding authors: Li-Li Ren (lily_ren@bjfu.edu.cn); Jiang-Li Tan (tanjl@nwu.edu.cn); Cornelis van Achterberg (kees@vanachterberg.org)

Received 6 June 2023

Accepted 15 October 2023

Published 2 November 2023

Academic Editor Martin Fikáček

Citation: Ge SX, Jiang ZH, Ren LL, van Achterberg C, Tan JL (2023) New insights into the phylogeny of Stephanidae (Hymenoptera: Apocrita), with a revision of the fossil species. *Arthropod Systematics & Phylogeny* 81: 819–844. <https://doi.org/10.3897/asp.81.e107579>

Abstract

The family Stephanidae (Hymenoptera) constitutes a unique group within the Apocrita, playing a pivotal role in the evolution of parasitoid wasps. Although the phylogeny of Stephanidae has been previously inferred, it remains at a low resolution when considering both extinct and extant genera, as well as the enigmatic extinct genus †*Electrostephanus*. Here, we undertake a revision of Stephanidae extinct, presenting descriptions of new specimens from late Cretaceous Burmese amber and early Eocene Baltic amber. Combining all extant and extinct genera, the phylogeny of Stephanidae was analyzed, incorporating 57 species within 21 genera based on 64 morphological characters. We apply both under maximum parsimony with equal weighting and implied weighting methods, with four species representing early Apocrita as outgroups. Divergence times are estimated by utilizing extinct taxa as calibration points. A new basal subfamily of stephanid wasp, †Lagenostephaninae **subf. nov.** was established, encompassing †*Lagenostephanus* and the newly described genera †*Tumidistephanus* **gen. nov.** and †*Neurastephanus* **gen. nov.** The genus †*Electrostephanus* is redefined, with two species assigned under distinct genera, †*Neurastephanus* **gen. nov.** and †*Aphanostephanus* **gen. nov.** We discuss some of the putative morphological synapomorphies of evolutionary significance within the phylogenetic framework. Our results complement several characteristics of great taxonomic importance for Stephanidae and provide new insights into the early evolution of the family.

Keywords

Cretaceous, Eocene, new genus, new subfamily, parasitoid wasps, systematics, taxonomy

1. Introduction

The crown wasp family Stephanidae Leach, 1815 (Hymenoptera: Apocrita: Stephanoidea) is a rare group of idiobiont ectoparasitoids, comprising 368 extant and 14 extinct species (Taylor 1967; Aguiar and Janzen 1999; van

Achterberg 2002; Aguiar 2004, 2006; Engel and Huang, 2016; Binoy et al., 2020; Ge et al., 2021a, 2021b, 2022; this study). Extant Species of Stephanidae are generally parasitoids of xylem boring beetles, including species

of Buprestidae, Cerambycidae, and even Curculionidae, but also hymenopterous larvae of Siricidae (Chao 1964; Taylor 1967; Kirk 1975; Königsman 1978; van Achterberg 2002; Aguiar 2004). The extant stephanids are of world wide distribution but occur mainly in subtropical and tropical regions (van Achterberg 2002; Aguiar et al., 2010; Hong et al., 2010, 2011; Chen et al., 2016; Tan et al., 2015a, 2015b, 2018), while the fossil records are limited and mostly derived from amber deposits in Myanmar (Cretaceous) and the Baltic region (Eocene), with only one Late Eocene compression fossil species, †*Protostephanus ashmeadi* Cockerell, 1906 from Colorado, USA (Aguiar and Janzen 1999; Engel and Ortega-Blanco, 2008; Li et al., 2017; this study).

Over the past two centuries, the small yet challenging family Stephanidae has garnered the attention of many researchers (Aguiar 2004). However, its phylogenetic position within Hymenoptera and its intergeneric classification remain contentious (Aguiar and Sharkov 1997; Aguiar 2001; van Achterberg 2002; Aguiar 2004). Before being recognized as a family, crown wasps were categorized as belonging to Ichneumonidae, Braconidae, and Evanoidea (Zschach 1788; Fabricius 1804; Jurine 1807). Leach (1815) erected the family Stephanidae under the superfamily Ichneumonoidea and included the Ichneumonid genus *Xorides*. Benoit (1949) initially proposed that stephanids constitute a separate superfamily (Stephanoidea). Subsequently, Rasnitsyn (1969) correctly delimited them and excluded “Stenophasmidae” (Braconidae) from the Stephanoidea. Vilhemsén (1997) asserted that the superfamily Stephanoidea, comprising the sole extant family Stephanidae, was the most basal group of Apocrita (Hymenoptera). Recent molecular analyses, however, have indicated that Stephanoidea + Evanoidea form a sister clade to the Trigonalioidea + Aculeata clade (Branstetter et al., 2017; Peters et al., 2017).

Regarding the intergeneric phylogeny of Stephanidae, van Achterberg (2002) initially proposed a phylogenetic chronogram of extant genera. Subsequently, Engel (2005) and Li et al. (2017) delved into the phylogeny of Stephanidae by incorporating both extant and extinct taxa. However, as a group of parasitoids is considered extremely rare (and even more so in the case of fossils), limited examination of specimens still undermines the understanding of the phylogenetic relationships within this group. Similar issue is more prominent in extinct groups. Some species from different lineages have been included in the genus †*Electrostephanus* (the type genus of the subfamily †Electrostephaninae) (van Achterberg 2002; Engel and Ortega-Blanco, 2008; Li et al., 2017), and many extinct taxa share common problems, including inaccurate original descriptions, a lack of available characteristics, poor preserved conditions, and missing type specimens (Aguiar and Janzen 1999; Engel 2005; Engel and Ortega-Blanco 2008; Li et al., 2017).

Here, a crown wasp preserved in mid-Cretaceous amber from Myanmar has been included in a new genus, †*Tumidistephanus* **gen. nov.**, and a new species †*T. prometheus* **sp. nov.** has been described. Another specimen preserved in Eocene Baltic amber is also newly described

and named †*Denaestephanus chaofeng* **sp. nov.** A third specimen in Baltic amber is attributed to †*Electrostephanus brevicornis* Brues, 1933 and designated as a neotype because Brues' holotype (formerly held at Albertus Universität, Königsberg) was destroyed at the end of World War II. Based on key morphological and chronological information provided by these specimens, the phylogeny of all extinct and extant genera of Stephanidae was inferred. We also inferred a dated phylogenetic tree to estimate the diversification times of Stephanidae and its main clades.

The aims of this study were as follows: (1) to describe the newly discovered fossil specimens of Stephanidae, (2) to investigate the phylogeny of Stephanidae using newly discovered and known specimens, and (3) to discuss the evolutionary implications within Stephanidae based on the phylogenetic analyses.

2. Material and methods

2.1. New material examined

Amber deposits containing †*Tumidistephanus prometheus* **sp. nov.** are located in the Hukawng valley, Tanai township, Myitkyina district of Kachin state, Myanmar (formerly Burma). The two Eocene fossil specimens (the neotype of †*Electrostephanus brevicornis* Brues, 1933 and †*Denaestephanus chaofeng* **sp. nov.**) studied here are from Samland or Kaliningrad Peninsula, situated along the Baltic coast. The types described in this paper have been deposited in the College of Forest Protection, Beijing Forestry University (BFU), China, and are part of Si-Xun Ge's collection (all new fossil specimens are available for re-examination by any researcher on request to Si-Xun Ge). All specimens were examined and photographed using a Canon G9 camera mounted on an Olympus CX31 microscope. Hand-sketched graphics were drawn using Adobe Photoshop CS6, and the final plates were prepared in Adobe Photoshop CC. The terminology follows Engel and Grimaldi (2004) and Engel et al. (2013), including the abbreviations for the wing venation as shown in Fig. 3A. The digital version of all figures in high resolution can be found in Zenodo archive under the following doi: <https://doi.org/10.5281/zenodo.8409208>.

2.2. Phylogenetic analysis: taxon sampling

Fifty-seven species of Stephanidae were selected as in-group taxa, representing all 10 extant and 11 extinct genera. Four additional species were selected as outgroups, based on the previously published phylogeny of Hymenoptera and fossil records of Stephanoidea (Sharkey et al., 2012; Li et al., 2013; 2015; 2017; Shih et al., 2017; Jouault et al., 2021). Detailed information regarding these taxa is provided in Supplementary Table S1.

2.3. Morphological characters observation and comparison

Morphological characteristics were observed by the first author or inferred from the literature: For extant taxa, species with specimens available for examination in the author's collection or well described in the literature were selected for phylogenetic analysis; For extinct taxa, based on a series of literature descriptions (Aguiar and Janzen, 1999; Engel and Grimaldi, 2004; Engel 2005; Engel and Ortega-Blanco, 2008; Engel et al., 2013; Engel and Huang, 2016; Li et al., 2017; Engel, 2019), pictures, and new specimens, 13 out of 14 extinct Stephanidae species were used for phylogenetic analysis (*†Danaeostephanus tridentatus* was excluded from the analysis due to the superficial original description and insufficient information in subsequent literature). Some characters were adopted or modified from those utilized by Li et al. (2017), Rasnitsyn and Zhang (2010) and van Achterberg (2002); modification was follows the suggestions in Simões et al. (2017). Inapplicable characters were represented as ‘–’ and unknown or missing characters were represented as ‘?’; morphological data were encoded using Mesquite 3.04 (Maddison and Maddison 2011). In total, 64 morphological characters (36 binary states and 28 multistate) were encoded as follows:

2.3.1. Head (Fig. 1)

1. Head, with coronal tubercles around front ocellus: (0) absent; (1) distinctly developed as 3–5 teeth (Fig. 1B, C); (2) developed as 7 teeth or more (Fig. 1A).
2. Ocelli: (0) gathered closely on vertex; (1) separated, with lateral ocelli almost reaching compound eyes (Fig. 1B); (2) separated, with distinct space between the lateral ocelli and compound eyes (Fig. 1C).
3. Antennae, flagellum: (0) short and robust, flagellomere with its length less than $2.4\times$ its maximum width; (1) elongated and slender, flagellomere with its length more than $2.7\times$ its maximum width.
4. Ivory streak behind eye (van Achterberg, 2002: 12): (0) absent; (1) present.
5. Vertex, median groove: (0) absent (Fig. 1B); (1) present (Fig. 1C).

2.3.2. Mesosoma (Fig. 2)

6. Pronotum length in the dorsal view (modified from Li et al, 2017: 22): (0) less than $0.8\times$ the maximum width (Fig. 2F); (1) $0.9\text{--}1.1\times$ the maximum width; (2) $1.2\text{--}2\times$ the maximum width (Fig. 2G, H).
7. Anterior part of pronotum (modified from van Achterberg, 2002: 14): (0) not elongated and modified as a distinct narrowed part (*i.e.* “neck” in van Achterberg (2002) and “colo” in Aguiar (1998); Fig. 2E); (1) elongated and modified as a distinct narrowed part developed (Fig. 2A–D).
8. The anterior part of the pronotum with its apex (van Achterberg, 2002: 20): (0) without an upcurved anterior flange or rim (Fig. 2D); (1) with an upcurved anterior flange or rim (Fig. 2A–C).

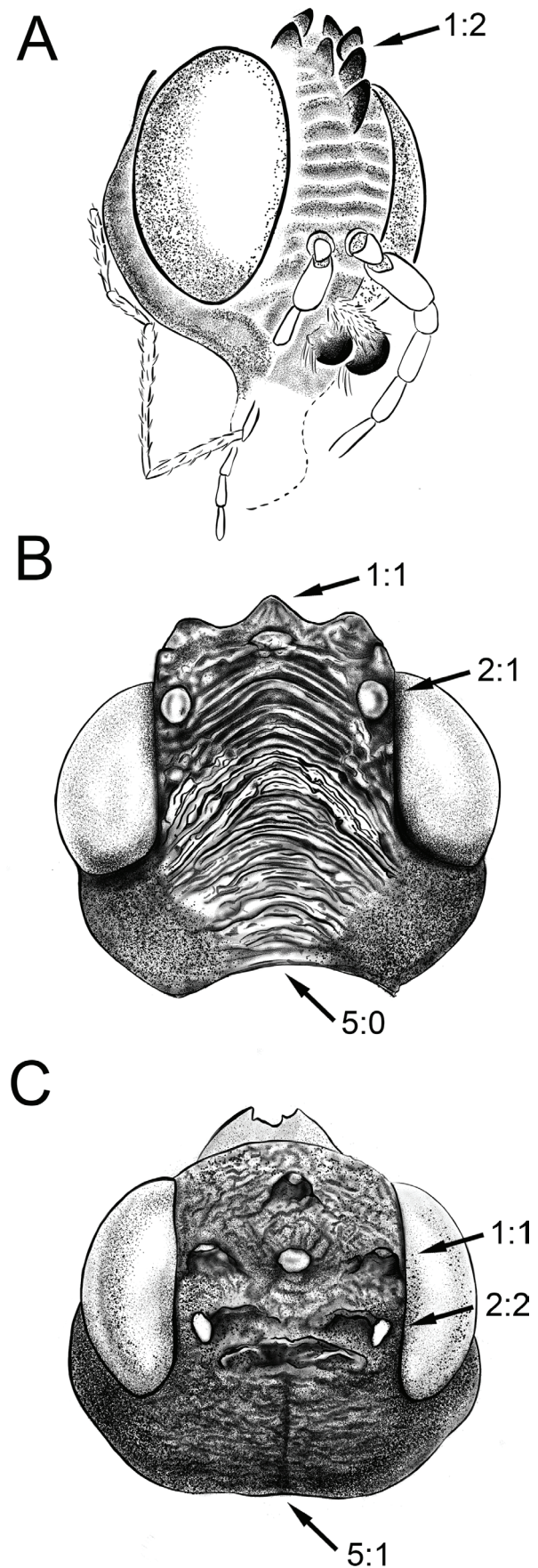


Figure 1. Head. **A** Anterior-oblique view of *K. zigrasi* Engel and Grimaldi; **B** dorsal view of *M. baogong* Ge and Tan; **C** dorsal view of *P. bimaculatus* Soliman, Gadallah and Dhafer. Character numbers and states are indicated by arrows (and so forth for other figures).

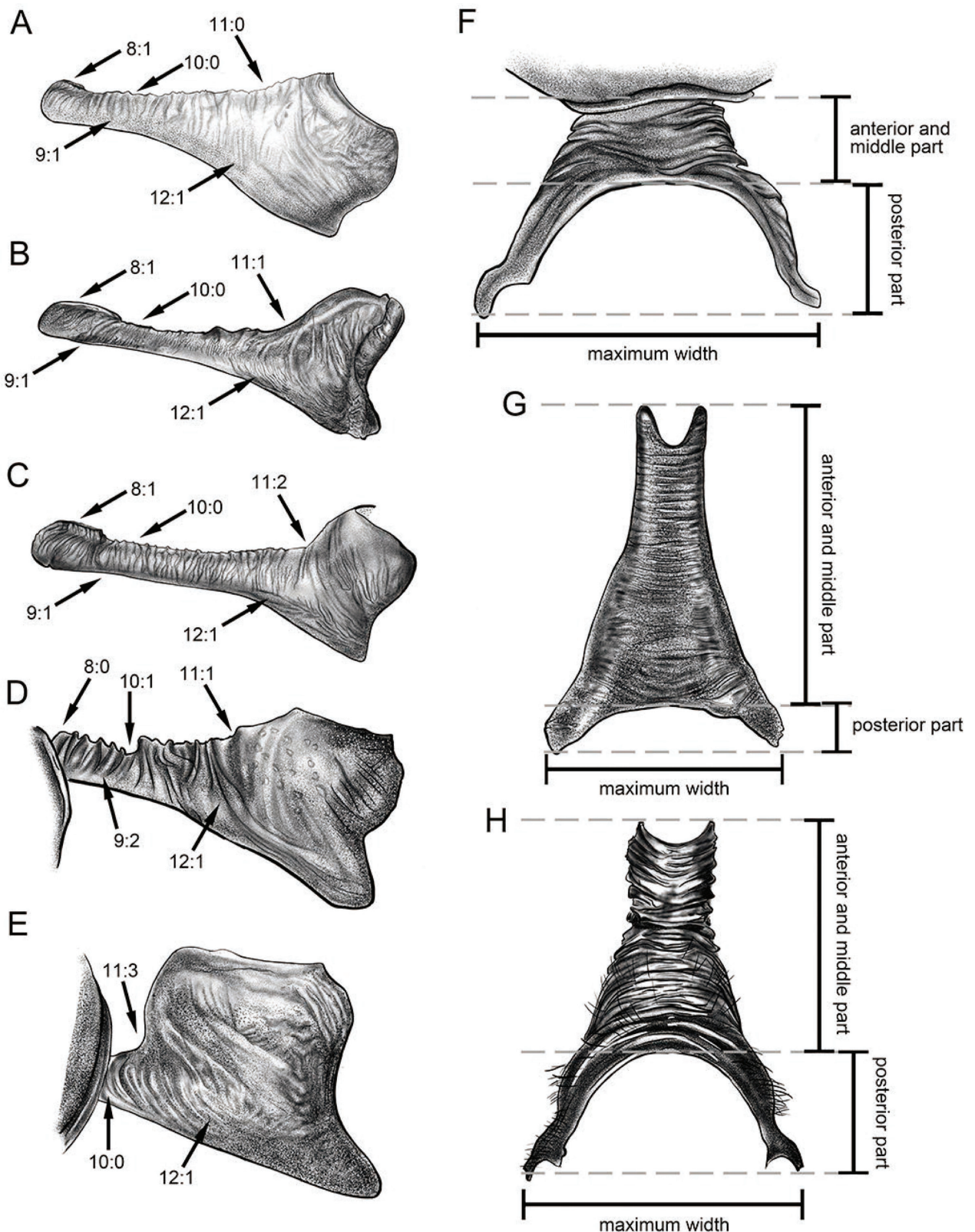


Figure 2. Pronotum, lateral view for (A–E) and dorsal view for (F–H); **A** *F. ruficollis* (Enderlein); **B** *F. andamanensis* Binoy, Girish Kumar and Dubey; **C** *F. chinensis* (Elliott); **D, H** *M. baogong* Ge and Tan; **E, F** *S. cinctipes* (Cresson, 1880); **G** *F. meridionalis* Ge and Tan.

9. Anterior half of pronotum with surface sculpture: (0) smooth; (1) weakly rugose (Fig. 2A–C); (2) distinct carinate (Fig. 2D–F).
10. Neck with its height viewed from the lateral view: (0) at the same level as the middle part of the pronotum

- (Fig. 2A–C); (1) at a somewhat lower level than the middle part of the pronotum (Fig. 2D).
11. Pronotum with its posterior part height viewed from the lateral view: (0) about the same level as the middle part of pronotum (Fig. 2A); (1) slightly ascending

at a somewhat higher level than the middle part of pronotum (at 135–150 degrees angle to the middle part) (Fig. 2B, D); (2) sloping ascend as a distinctly higher level than the middle part of pronotum (at 100–120 degrees angle to the middle part) (Fig. 2C); (3) vertically elevated as a distinctly higher level than the middle part of pronotum (almost perpendicular to the middle part) (Fig. 2E).

12. Pronotum with its surface sculpture in the middle and posterior parts: (0) smooth or coriaceous; (1) rugosity (Fig. 2A–E).
13. Pronotum with the length of its anterior and middle part in the dorsal view (modified from Li et al, 2017: 22): (0) shorter than 0.9× the posterior part (Fig. 2F); (1) 0.9–1.2× the posterior part; (2) 1.3–2.5× the posterior part (Fig. 2H), and (3) longer than 2.5× the posterior part (Fig. 2G).

2.3.3. Wings (Fig. 3)

14. Hindwing, vein Cu-a (Li et al., 2017: 16): (0) present (Fig. 3A); (1) absent (Fig. 3B–H).
15. Hindwing, vein M+Cu: (0) complete or basally present (Fig. 3A, D); (1) absent (Fig. 3B, C, E–H).

16. Wing fixation apparatus (cenchri + rough area within a loop of 2A vein) (Rasnitsyn and Zhang, 2010: 3): (0) present; (1) absent (Fig. 3 A–H).
17. Forewing, vein 3r-m (Rasnitsyn and Zhang, 2010: 9): (0) present; (1) absent.
18. Forewing, vein 2r-m: (0) present; (1) absent.
19. Forewing, vein 2m-cu (Rasnitsyn and Zhang, 2010: 10): (0) present; (1) absent.
20. Forewing, vein 2Cu_b (modified from Li et al., 2017: 9): (0) present and sclerotized (Fig. 3A); (1) nebulous or pigmented (Fig. 3G, H); (2) absent (Fig. 3B, C).
21. Forewing, vein Rs+M (modified from Li et al., 2017: 2): (0) present and sclerotized (Fig. 3A, B, D–G); (1) nebulous or pigmented (Fig. 3H); (2) absent (Fig. 3C).
22. Forewing, vein 2-Rs (modified from Li et al., 2017: 2): (0) present and sclerotized (Fig. 3A, B, D–G); (1) nebulous or pigmented (Fig. 3H); (2) absent (Fig. 3C).
23. Forewing, vein apical abscissa of vein M (modified from Li et al., 2017: 2): (0) reduced or pigmented (Fig. 3B, H); (1) complete and sclerotized (Fig. 3A, D–G); (2) absent (Fig. 3C).

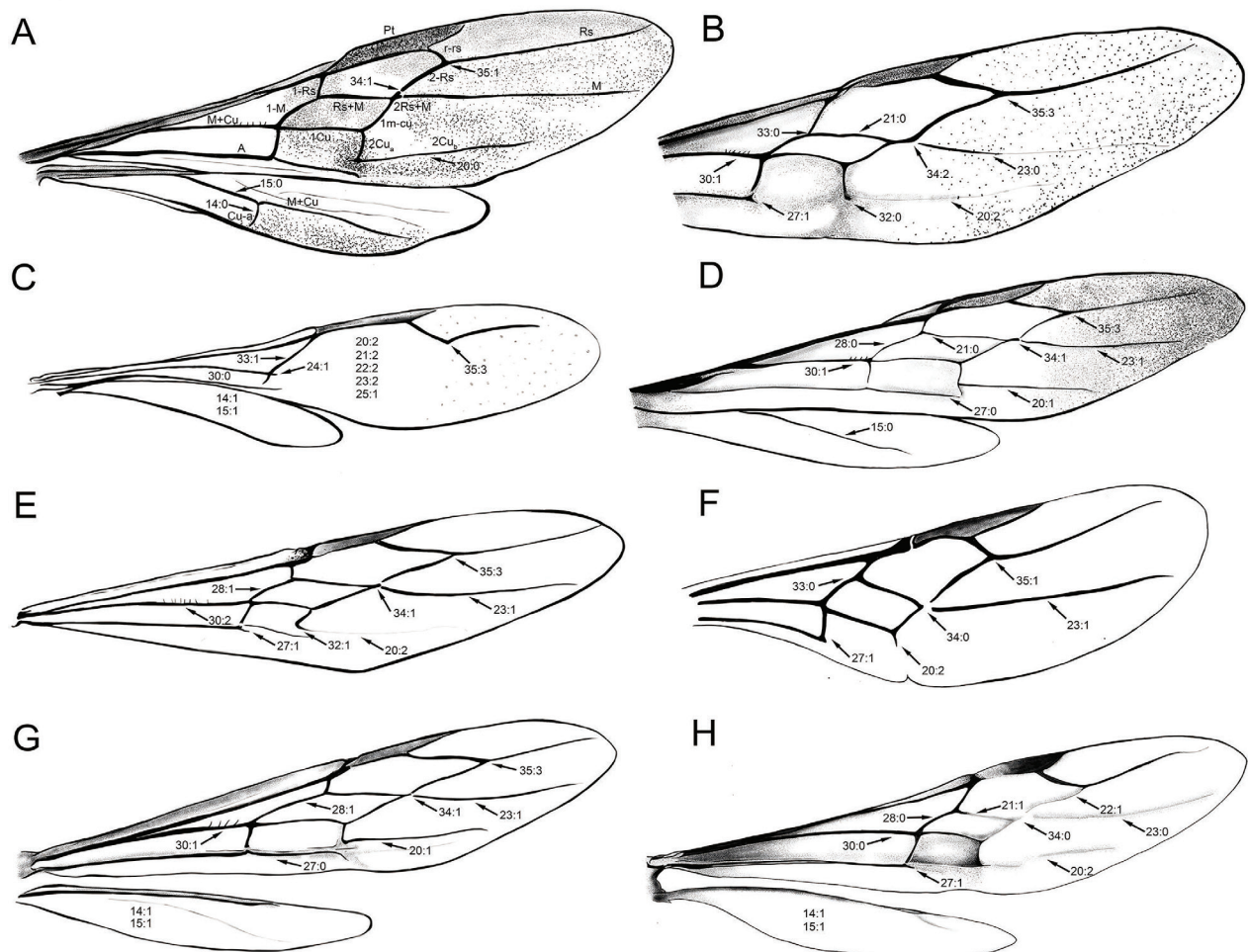


Figure 3. Wings. **A** *S. determinatoris* Madl; **B** *P. matsumotoi* van Achterberg; **C** *F. meridionalis* Ge and Tan; **D** *A. gigas* (Schletterer); **E** *H. macrurus* (Schletterer); **F** *K. zigrasi* Engel and Grimaldi; **G** *M. baogong* Ge and Tan; **H** *P. bimaculatus* Soliman, Gadalalah and Dhafer.

24. Forewing, vein 1Cu (modified from Li et al., 2017: 2): (0) completely developed, connecting to 1m-cu and 2Cu_a (Fig. 3A, B, D–H); (1) absent or only basally present (Fig. 3C).
25. Forewing, vein 1m-cu (modified from Li et al., 2017: 2): (0) present (Fig. 3A, B, D–H); (1) absent (Fig. 3C).
26. Forewing, vein 2Rs+M: (0) longer than 0.8× the vein 1-Rs (Fig. 3B); (1) 0.4–0.8× the vein 1-Rs (Fig. 3G); (2) shorter than 0.4× the vein 1-Rs (Fig. 3A).
27. Forewing, vein A (modified from Li et al., 2017: 11): (0) complete, beyond Cu-a (Fig. 3A, D, E); (1) incomplete, only reached Cu-a or was lost (Fig. 3B, C).
28. Forewing, vein 1-M: (0) curved distally (Fig. 3A, B, D); (1) straight (Fig. 3E, G).
29. Forewing, vein 1-Rs: (0) curved distally; (1) straight.
30. Forewing, spiny setae on vein M+Cu: (0) absent (Fig. 3C, H); (1) developed distally near the base of vein 1Cu (Fig. 3A, B, D, G); (2) developed medially, far from the base of vein 1Cu (Fig. 3E).
31. Forewing, with terminal part of vein A (modified from van Achterberg, 2002: 16): (0) curved downwardly; (1) straight.
32. Forewing, 2Cu_a: (0) vertically or sub-vertically developed (Fig. 3A, B, G, H); (1) strongly reclivous basally (Fig. 3E).
33. Forewing, vein 1-Rs and 1-M: (0) distinctly angled (Fig. 3A, B, D–H); (1) developed as a straight line (Fig. 3C).
34. Forewing at the junction of 2-Rs, M, and 2Rs+M: (0) obvious disconnection with distinct space (Fig. 3F, H); (1) slight incision (Fig. 3A, D, E, G); (2) at least with 2-Rs and 2Rs+M combined (Fig. 3B).
35. Forewing with a vertical position of apical 2r-rs (in Stephanidae = r-rs): (0) near the middle of pterostigma (modified from Li et al., 2017: 6); (1) between middle and apical of pterostigma (Fig. 3A, F); (2) at the apical of pterostigma; (3) extending beyond apical of pterostigma (Fig. 3B–E, G, H).
36. Forewing, vein Rs+M and 1Cu: (0) parallel (Fig. 3A, B, D–H); (1) nonparallel.
37. Forewing, vein 1-M (modified from Li et al., 2017: 3): (0) shorter than 2.8× the vein 1-Rs (Fig. 3A, B, H); (1) 2.8–3.6× the vein 1-Rs; (2) longer than 3.6× the vein 1-Rs (D–G).
38. Forewing, vein 1-M: (0) shorter than 1.4× the vein 1m-cu (Fig. 3A–H); (1) 1.4–1.7× the vein 1m-cu; (2) longer than 1.7× the vein 1m-cu.
39. Forewing, vein 2-Rs: (0) shorter than 1.8× the vein 2r-rs (in Stephanidae = r-rs) (Fig. 3B–E, G, H); (1) longer than 1.8× the vein 2r-rs (in Stephanidae = r-rs) (Fig. 3A, F).
40. Forewing with a vertical position of vein 1m-cu apical ends (modified from Li et al., 2017: 12): (0) near the ends of 2Cu_a or slightly extended (Fig. 3A, B, F, H); (1) distinctly extended beyond the ends of 2Cu_a (Fig. 3D, E, G).
41. Forewing with angle between 1-M and 1Cu (modified from Li et al., 2017: 12): (0) greater than 55° (Fig. 3A, B, F, H); (1) lesser than 55° (Fig. 3D, E, G).

2.3.4. Legs (Fig. 4)

42. Front tibia cross-section shape: (0) tubular; (1) more or less dorsoventrally flattened.
43. Front tibia, with row of dorsal teeth: (0) absent; (1) present.
44. Hind coxa, maximum length in lateral view: (0) less than 2.5× its basal width (Fig. 4A); (1) 2.6–4× its basal width (Fig. 4B); (2) longer than 4× its basal width.
45. Hind coxa with surface sculpture: (0) smooth or coriaceous; (1) rugose (Fig. 4A, B).
46. Hind coxa, dorsal teeth (van Achterberg, 2002: 5): (0) absent (Fig. 4B); (1) present (Fig. 4A).
47. Hind femur with surface sculpture: (0) largely smooth (Fig. 4B); (1) sparsely granulated (Fig. 4A); (2) completely coriaceous.
48. Hind femur with its maximum length in lateral view: (0) less than 3× its maximum width (Fig. 4B); (1) 3–4× its maximum width (Fig. 4A); (2) 4–5× its maximum width; (3) longer than 5× its maximum width.
49. Hind femur (modified from Li et al., 2017: 25): (0) without ventral dentition; (1) quadridentate with four or more large teeth ventrally; (2) tridentate with three main teeth ventrally (Fig. 4A); (3) bidentate with two large teeth ventrally (Fig. 4B).
50. Hind femur with minor teeth between large teeth (modified from Li et al., 2017: 25): (0) absent, (1) weakly developed (Fig. 4A, B), and (2) strongly developed.
51. Hind femur with length: (0) shorter than 0.8× the hind tibia (Fig. 4A); (1) longer than 0.8× the hind tibia (Fig. 4B).
52. Depression at the inner side of the hind tibia (modified from van Achterberg, 2002: 6): (0) absent (Fig. 4A); (1) incompletely developed as oblique groove (Fig. 4B); (2) completely developed as pit-like shape (Fig. 4C); (3) deeply developed as distinct V-shaped (Fig. 4D); (4) developed as shallow V-shaped (Fig. 4E).
53. Hind tibia, maximum width (modified from van Achterberg, 2002: 7): (0) shorter than 1.7× its basal width; (1) 1.7–2.5× its basal width (Fig. 4A, C–E); (2) 2.5–3.5× its basal width (Fig. 4B); (3) longer than 3.5× its basal width.
54. Hind tarsus of females (van Achterberg, 2002: 9): (0) 5-segmented (Fig. 4A); (1) 3-segmented (Fig. 4B, E).
55. Hind tarsus length of the basitarsus: (0) shorter than 2× the second tarsomere; (1) 2–3× the second tarsomere; (2) 3–4× the second tarsomere; (3) longer than 4× the second tarsomere.

2.3.5. Metasoma (Fig. 5)

56. First metasomal sternite (van Achterberg, 2002: 3): (0) not fused with the first tergite; (1) immovably joined to the first tergite.
57. The first metasomal segment with length in dorsal view: (0) shorter than 1.5× its maximum width; (1) 2–4× its maximum width (Fig. 5B); (2) 4–6× its maximum width; (3) longer than 6× its maximum width (Fig. 5A).

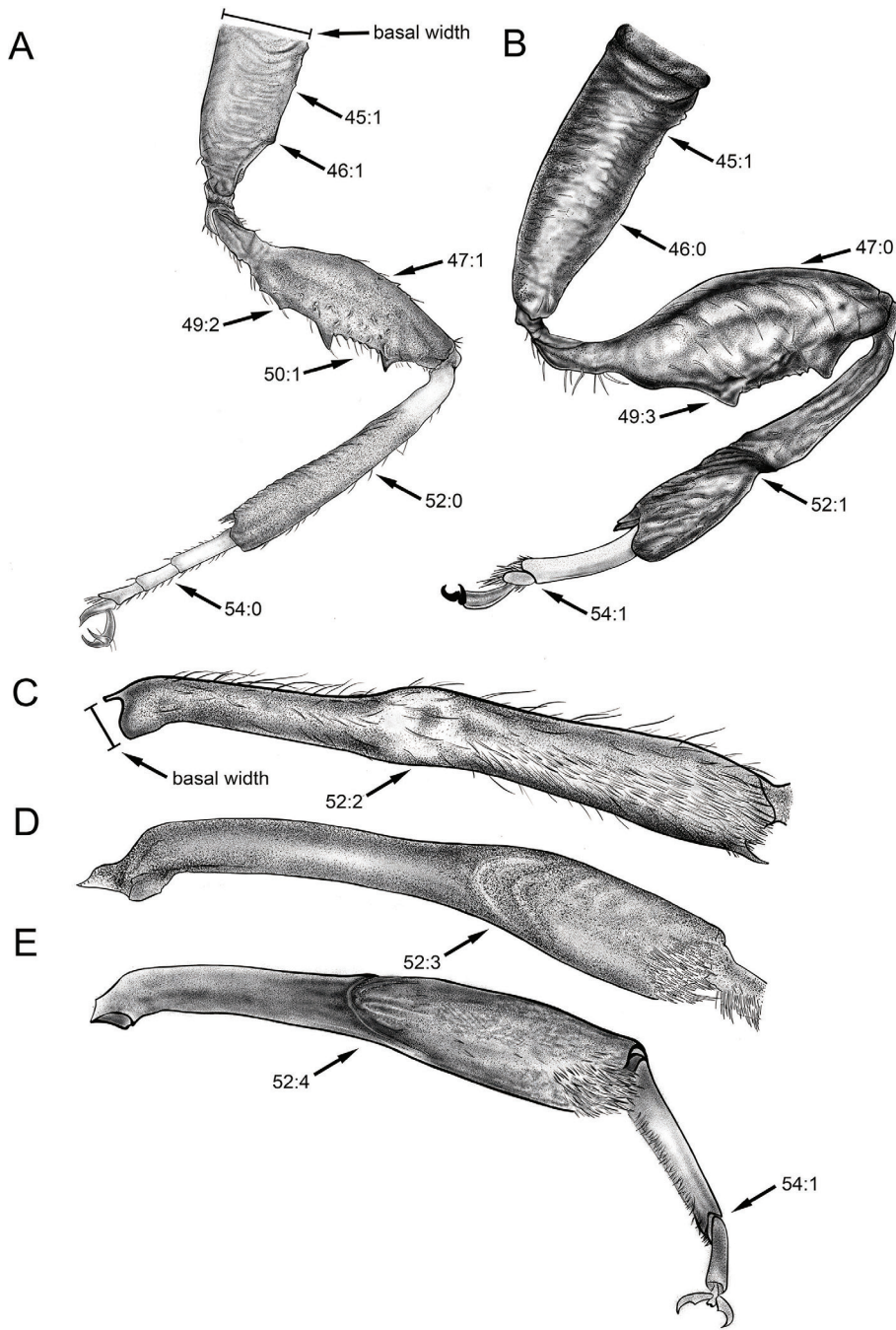


Figure 4. Hind legs. **A** *S. determinatoris* Madl; **B** *P. notiochinensis* Tan and van Achterberg; **C** *M. baogong* Ge and Tan (only the tibia is shown); **D** *F. meridionalis* Ge and Tan (only tibia is shown); **E** *P. bimaculatus* Soliman, Gadallah and Dhafer (only tibia and tarsus are shown).

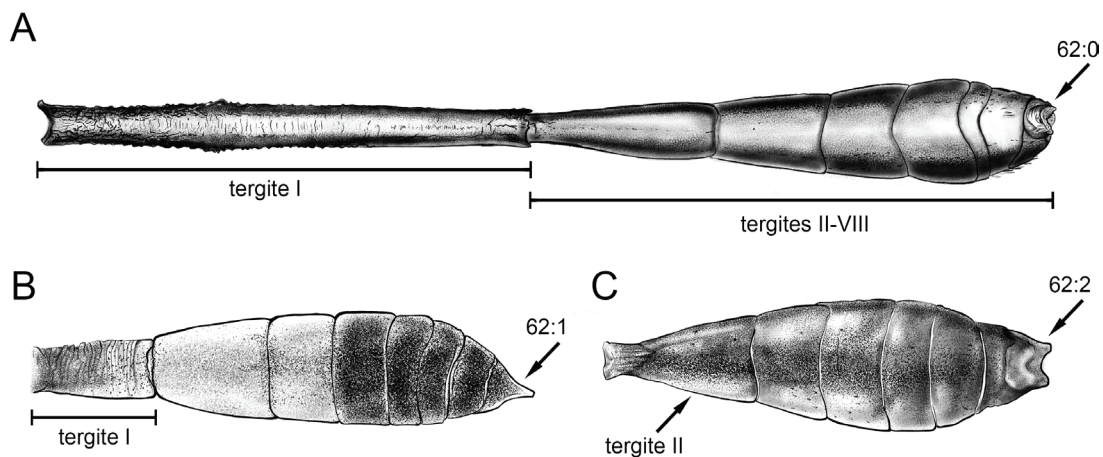


Figure 5. Metasoma. **A** *M. baogong* Ge and Tan; **B** *S. cinctipes* (Cresson); **C** *P. matsumotoi* van Achterberg (only tergite II–VIII are shown).

58. First metasomal segment length relative to second metasomal segment (modified from Li et al., 2017: 30): (0) nearly as long as the second metasomal segment (Fig. 5B); (1) longer than the second metasomal segment but shorter than 0.5× metasoma except first segment; (2) as long as 0.6–0.8× metasoma except first segment (Fig. 5A); (3) approximately 0.9× as long as metasoma except first segment or longer.
59. First metasomal segment width relative to second metasomal segment: (0) first segment similar to the second segment; (1) first segment distinctly narrower than second segment.
60. First metasomal segment surface sculpture: (0) smooth or coriaceous; (1) rugose
61. Second and subsequent metasomal segments: (0) not forming a distinct unity; (1) forming a distinct unity.
62. Female, pygidial area (modified from van Achterberg, 2002: 22): (0) weakly developed as inconspicuous protrusions (Fig. 5A); (1) distinctly developed with pygidial horns (Fig. 5B); (2) deeply V-shaped depressed (Fig. 5C).
63. Ovipositor sheath with a whitish subapical band (van Achterberg, 2002: 1): (0) absent; (1) present.
64. Ovipositor (modified from Li et al., 2017: 32): (0) hardly surpassing apex of metasoma at rest; (1) approximately as long as metasoma; (2) approximately as long as body.

2.4. Phylogenetic analysis

Phylogenetic trees were generated under the maximum parsimony (MP) criterion, along with an implied weighting (IW) analysis. The optimal concavity constant value (K -value) required for IW analysis was calculated using a TNT script `setk.run` (Santos et al., 2015). The K -value assigns weights to characters based on their degree of homoplasy (the lower the value of K , the higher the strength against homoplasy) (Legg et al., 2013) thereby enhancing the quality of phylogenetic results (Goloboff et al., 2008). Additionally, an equal weighting (EW) analysis was conducted with TNT v.1.1 (Goloboff et al., 2008) incorporating new technology analysis (Sectorial Search, Ratchet, Drift, and Tree fusing with default parameters). Unambiguous characters were mapped onto strict consensus trees using `Winclada v1.00.08` (Nixon, 2002). Node robustness was tested using both bootstrap (BS) values and absolute Bremer support values.

In the description section, we employed specific adverbs to convey the strength of support for each range of the BS: ‘weakly’ for values less than 20; ‘moderately’ for values greater than or equal to 20 but less than 50; ‘highly’ for values greater than or equal to 50 but less than 75, and ‘strongly’ for values greater than or equal to 75.

2.5. Divergence time estimation

The divergence time of Stephanidae was estimated using Bayesian inferences (BI) with a relaxed clock model in

MrBayes 3.2.7a (Huelsenbeck and Ronquist 2001; Ronquist and Huelsenbeck 2003; Ronquist et al., 2012), with all node topologies shown as monophyletic in the IW analysis constraint. We performed tip-dating analyses using a fossilized birth-death model, where fossil taxa were treated as terminals taxa. The analyses were computed with an `Mkv + G` unordered model (Lewis 2001) and an independent gamma relaxed clock model (Lepage et al., 2007; `lset rates = gamma, prset clockvarpr = IGR, prset igrvarpr = exp(10)`); no rate variation was computed with `lset rates = equal`). Following the approach described by Zhang and Wang (2019), we set the prior for the clock rate based on the results of previous non-clock analyses (`prset clockratepr = lognorm (-3.9120, 1.0202)`). The proportion of extant taxa was set to 0.028, considering that 10 extant genera contained approximately 368 extant species. The sampling strategy of taxa was set to diversity (`prset samplestrat = diversity` wherein fossils are sampled randomly and can be tips or ancestors). An exponential prior and beta prior were used for the net speciation rate and the relative extinction rate using the following functions: `prset speciationpr = exp (10)` and `prset extinctionpr = beta (1,1)`, respectively. In all our tip-dating analyses, the node age prior was set to “calibrated.” All analyses comprised four runs and six Markov chains Monte Carlo (MCMC) and were launched for 5 million generations. MCMC were sampled every 500 generations and a burn-in fraction of 0.25 was used. Tip-dating analyses were performed on the most extinct taxa calibrated with uniform distributions bounded according to the minimum and maximum ages of their deposits (Aguilar and Janzen 1999; Engel 2005; 2019; Engel and Ortega-Blanco 2008; 2013; Li et al., 2017), while †*Protostephanus* was calibrated with fixed distributions according to the original description (Cockerell 1906; Aguilar and Janzen 1999).

3. Results

3.1. Phylogeny

The IW analysis, with a K -value of 10.957032 calculated using the script `setk.run`, generated the three most parsimonious trees. These trees share congruent topologies, although some slight inconsistencies were noted for some terminal nodes (interspecific topological structures within *Megischus*, *Parastephanellus* and *Foenatopus*). The strict consensus tree (Fig. 6) had a length of 324 steps, a consistency index (CI) of 0.318, and a retention index (RI) of 0.770.

In the EW analysis, five most parsimonious trees were generated. These trees maintained consistent topologies at the genus level, with the exception of *Megischus* and *Hemistephanus*. A strict consensus tree (Supplementary Figure S1) derived from these trees had a length of 327 steps, a CI of 0.315, and a RI of 0.767. The topology was mostly identical to that obtained from the IW analysis,

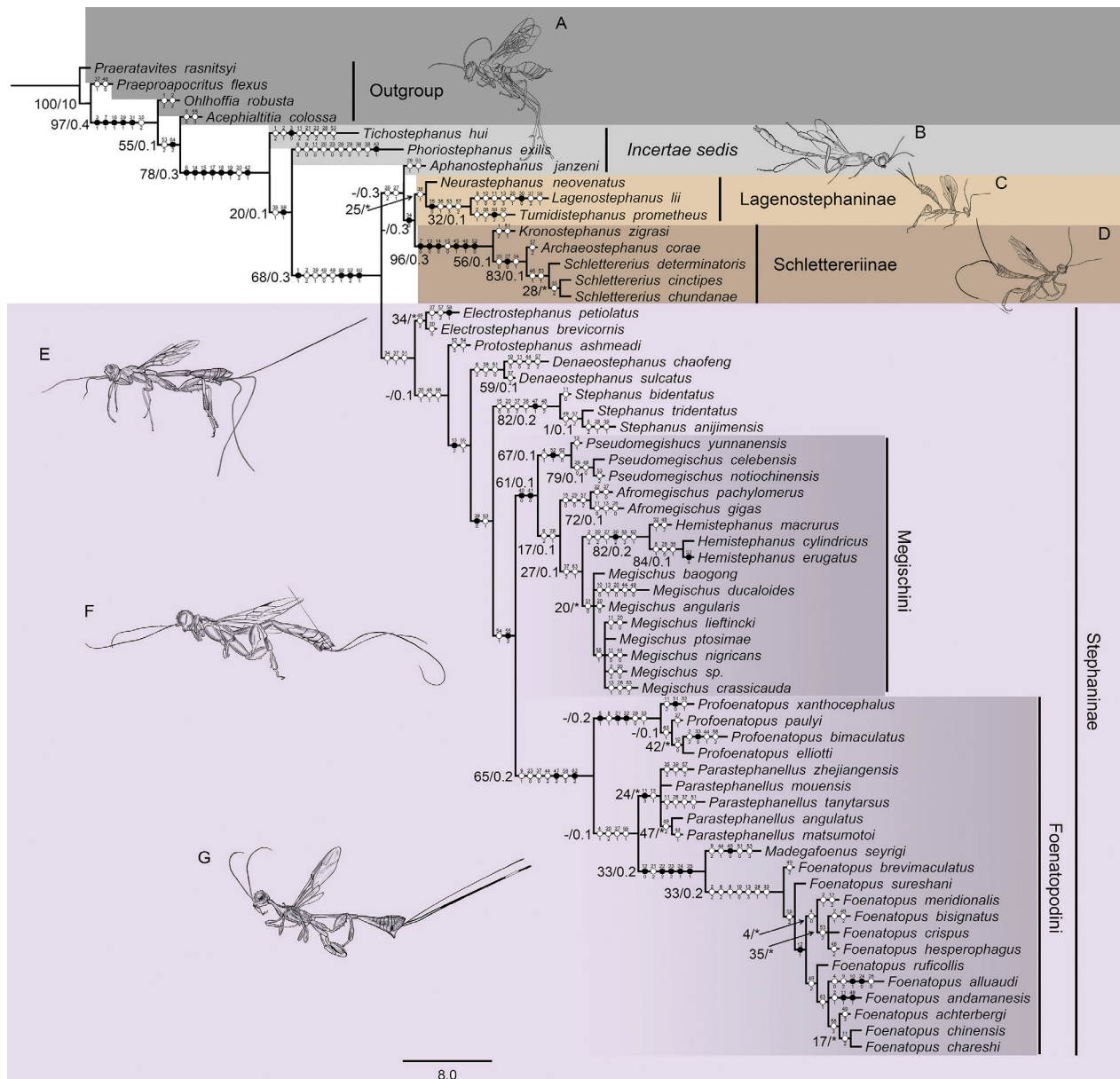


Figure 6. A strict consensus tree was obtained by implied weighting (IW). Solid bullets (●) indicate non-homoplastic synapomorphies; open bullets (○) indicate homoplastic characters. Bootstrap values (BS, shown as ‘-’ if absent) and Bremer support values (BR, shown as ‘*’ if absent) are separated by a slash ‘/’ and marked beside each node. **A** *O. robusta* Jouault, Rasnitsyn and Perrichot; **B** *T. hui* Engel; **C** *L. lii* Li, Rasnitsyn, Shih and Ren; **D** *S. chundanae* Tan and van Achterberg; **E** *S. anijimensis* Watanabe and van Achterberg; **F** *P. notiochinensis* Tan and van Achterberg; **G** *F. achterbergi* Gupta and Gawas.

except *Megischus* formed a paraphyletic group and clustered with the monophyletic genus *Hemistephanus* (in IW analysis both genera are monophyletic and sister to each other).

The following cladogram description is based on the strict consensus tree generated under IW analysis (Fig. 6).

3.1.1. †Lagenostephaninae subf. nov.

Monophyly of the †Lagenostephaninae **subf. nov.** was moderately supported (BS=25). Within †Lagenostephaninae, †*Neurastephanus neovenatus* **comb. nov.** was sister to †*Lagenostephanus lii* and †*Tumidistephanus prometheus* **sp. nov.** with the latter two forming a moderately supported monophyletic clade (BS=32).

3.1.2. Schlettereriinae

A sister group relationship between Schlettereriinae and †Lagenostephaninae was weakly supported. The monophyly of Schlettereriinae was strongly supported (BS=96). Within Schlettereriinae, †*Kronostephanus zigrafi* showed its unique sister lineage to †*Archaeostephanus corae* + *Schlettererius* as highly supported (BS=56). *Schlettererius* was moderately supported (BS=28) as a monophyletic clade.

3.1.3. Stephaninae

In Stephaninae, all genera were well supported as monophyletic. The inter-subfamily relationships are summa-

rized as follows: †*Electrostephanus*, †*Protostephanus*, †*Denaestephanus*, and *Stephanus* as successive sisters (Megischini + Foenatopodini). Megischini was highly supported (BS=61) as a monophyletic clade with *Pseudomegischus* sister to *Afromegischus* + (*Hemistephanus* + *Megischus*). Foenatopodini was highly supported (BS=65), with *Profoenatopus* sister to *Parastephanellus* + (*Madegafoenus* + *Foenatopus*)

3.1.4. *Incertae sedis*

A sister group relationship between †*Tichostephanus hui* and other Stephanidae was strongly supported (BS=75). †*Phoriostephanus exilis* was moderately supported as a sister to other Stephanidae species (BS=20). The clade of †*Aphanostephanus janzeni* **comb. nov.**, and †Lagenostephaninae **subf. nov.** + Schlettereriinae was weakly supported.

3.2. Divergence time estimation

As shown in the cladogram (Fig. 7), the divergence times of stem- and crown- Stephanidae were estimated at around 159.9 Ma (95% HPD = 150.5–169.2 Ma, Late Jurassic) and 155.4 Ma (95% HPD = 144.8–165.3 Ma, Late Jurassic to Early Cretaceous), respectively; the crown- Schlettereriinae originated at around 116.9 Ma (95% HPD = 101.7–133 Ma); †Lagenostephaninae diverged 126.2 Ma (95% HPD = 108.7–140.8 Ma) while the stem- Stephaninae diverged around 136.8 Ma (95% HPD = 119.5–153.6 Ma); the origin of the tribe Foenatopodini was estimated at around 97.6 Ma (95% HPD = 74.4–122.2 Ma) and the tribe Megischini at approximately 92.3 Ma (95% HPD = 65.9–117.2 Ma).

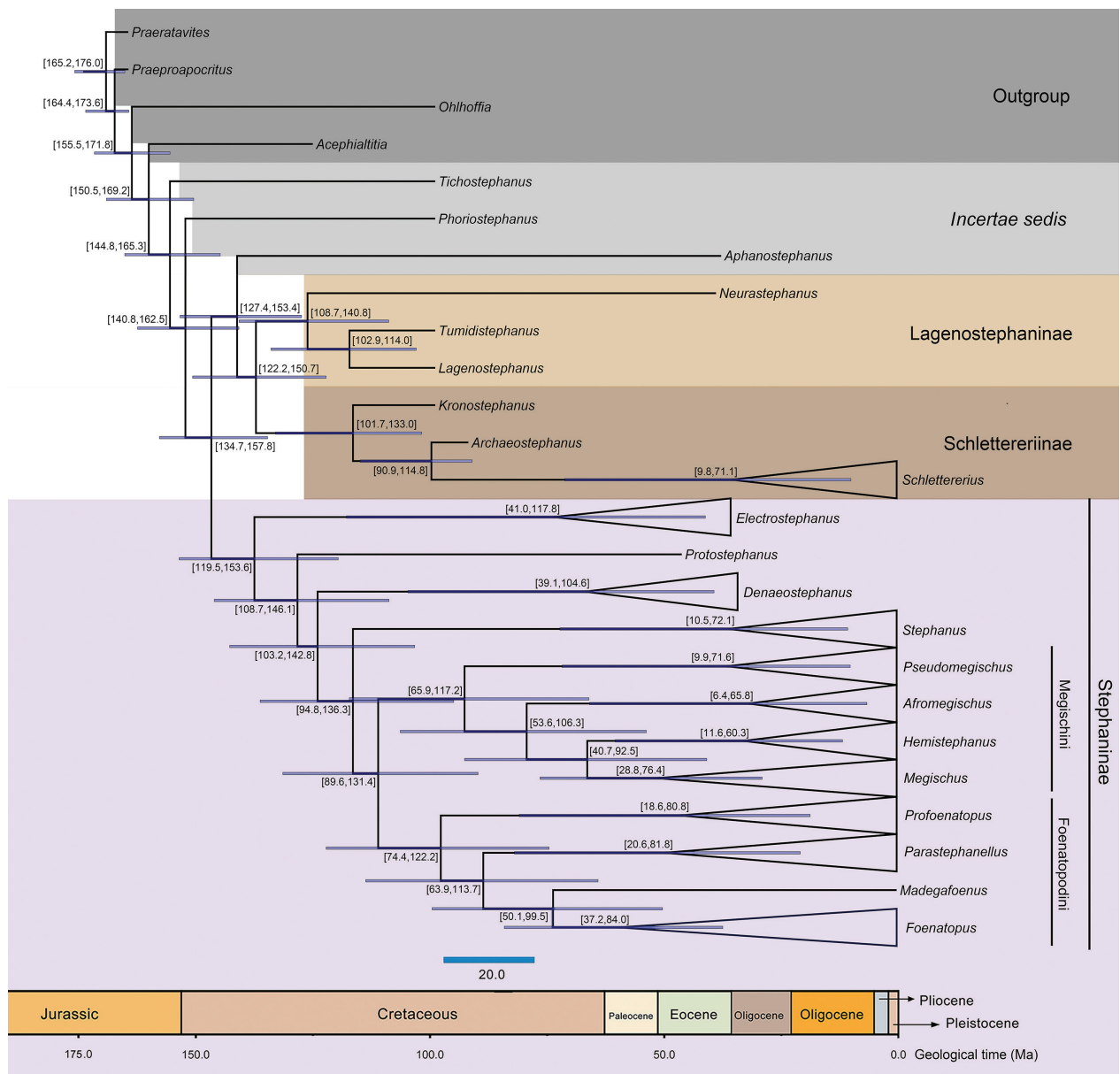


Figure 7. Time-calibrated phylogenetic relationships of Stephanidae genera generated by Bayesian inference, with monophyletic lineages constraint according to strict consensus tree obtained under implied weighting.

3.3. Taxonomy

Order Hymenoptera Linnaeus, 1758 Superfamily Stephanoidea Leach, 1815 Family Stephanidae Leach, 1815

Subfamily †Lagenostephaninae Ge and Tan, subf. nov.

<https://zoobank.org/2231D702-9DC0-4277-8E5B-75611E0C-BA24>

Type genus. †*Lagenostephanus* Li, Rasnitsyn, Shih and Ren, 2017

Diagnosis (see also Table 1). Pronotum elongated with neck differentiated. Pronotal fold present. Forewing with vein 1-M arched; vein r-rs as long as 1-Rs; vein Rs+M and 1Cu nonparallel; vein 2Rs + M differentiated, not connect with free abscissa of vein M and vein 2-Rs. Hind coxa largely smooth, without transverse rugose. Hind femur robust and coriaceous. Tergite I almost as long as tergite II. Ovipositor sheath about as long as metasoma.

Comments. The phylogenetic results indicated that the new subfamily forms a monophyletic group that sister to Schlettereriinae. When the characters are mapped on the tree, the new subfamily does not possess any unique synapomorphy, while its sister relationship to Schlettereriinae is supported by a synapomorphy (character 34: 0). This is caused by the male †*Neurastephanus neovenatus* which is revealed as member of †Lagenostephaninae based on forewing with vein 1-M 1.4–1.7× as long as vein 1m-cu (character 38: 1), the largely smooth hind coxa (character 45: 0), the forewing with vein 2Rs+M non-connecting to 2-Rs (character 34: 0), the apical abscissa of vein M (character 23: 1), and vein Rs+M of fore wing converging to vein 1Cu distally (character 36: 1). All above characters are homoplastic within Stephanidae. The length of ovipositor (characters 64), which is short in †Lagenostephaninae and represents the unique synapomorphy of the subfamily, cannot be coded for †*Neurastephanus neovenatus* and hence cannot be mapped in Fig. 6. Intriguingly, based on the comparatively short ovipositor and small body sizes of †Lagenostephaninae, we speculate that these may reflect a unique ecological niche of the lineage (e.g. possible parasitism of bark beetles) different from Schlettereriinae that are parasitoids of xylen borers. We believe it is hence reasonable to establish this lineage as a new subfamily rather than combine it with Schlettereriinae.

Genus †*Tumidistephanus* Ge and Tan, gen. nov.

<https://zoobank.org/B7654596-DFC3-4081-92B8-FB377ECB-3C3A>

Type species. †*Tumidistephanus prometheus* Ge and Tan, sp. nov.

Etymology. From “tumidi” (Latin for “swollen”) and the generic name, *Stephanus* Jurine. The name is an allusion to the robust hind femur and tibia of the type specimen. The gender of the name is masculine.

Diagnosis. Head elliptical (Fig. 8A). Mesosoma robust, pronotum with distinct U-shaped pronotal fold. Hind coxa rather strong with distinct lateral groove. Hind femur rather robust with its median part extremely swollen as nearly oval shaped (Fig. 8E). Hind femur with 2 large teeth and 10 medium sized teeth (4 of them between large teeth and 6 behind the apical large teeth). Hind tibia with two spurs and with its apical half rather dilated, almost as wide as hind femur. Hind tarsus of female 5-segmented. Forewing with Rs + M and 1Cu non-parallel (Fig. 8B); 2Rs + M rather elongated, almost as long as 1-Rs. Metasomal T1 and S1 not fused laterally. Ovipositor length almost as long as the metasoma.

†*Tumidistephanus prometheus* Ge and Tan, sp. nov.

<https://zoobank.org/65354276-42A3-42F2-9281-2B96E7553E-CA>

Figures 8–10

Holotype. ♀; BFU, Myanmar Amber, Cretaceous. Part of Si-Xun Ge’s collection.

Etymology. The species’ name is derived from the name Prometheus in ancient Greek mythology, who brought fire and knowledge to humans. We named the new species analogous to its discovery, bringing a new perspective on Stephanidae systematics.

Diagnosis. See generic diagnosis above.

Description. Female. Total body length (from head anterior to metasoma distal margin, without ovipositor sheath) 2.8 mm; forewing length 2.2 mm; Ovipositor sheath 1.05 mm. — **Head:** Antenna elongate, filiform with at least 19 flagellomeres; the first flagellomere robust and elongated, and second flagellomere relatively short; Head elliptical with compound eyes sub-triangular; vertex with five tubercles; temple distinctly narrowed behind eye; Maxillary palpus 5-segmented, elbowed between MP II (maxillary palpomere II) and MP III (maxillary palpomere III) with its basal two segments relatively short and robust, while apical three segments long and slender. — **Mesosoma:** Pronotum robust with U-shaped pronotal fold strongly developed; middle part of pronotum protuberant weakly differentiated from posterior part and at somewhat higher level. — **Wings:** Forewing with vein 1-M distinctly curved, 1.7× as long as vein 1-Rs and 2.1× vein 1m-cu; vein A incomplete, only

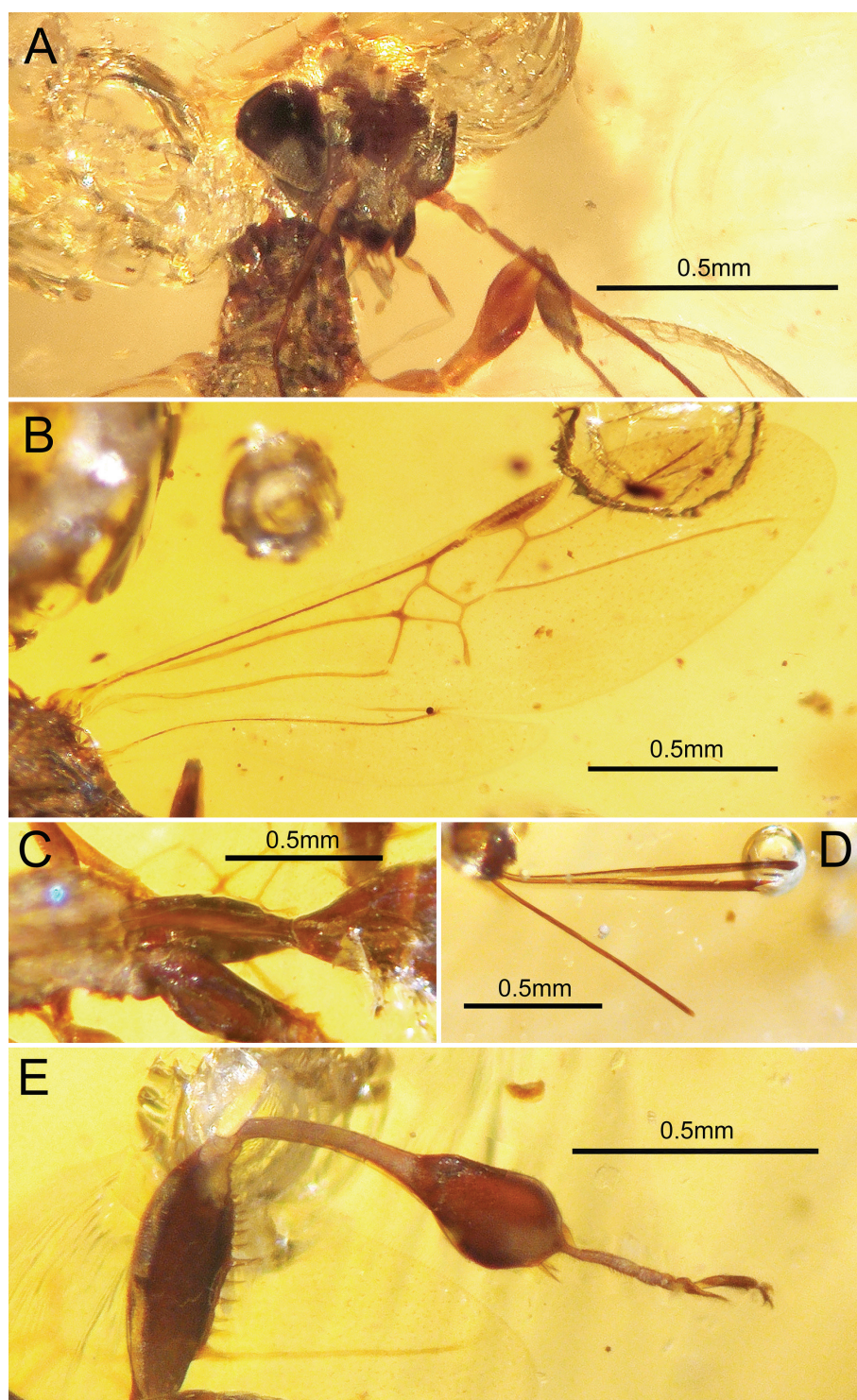


Figure 8. *Tumidistephanus prometheus* Ge and Tan, **sp. nov.** Holotype ♀. **A** Head, frontal view. **B** Wings. **C** Tergite I and II, lateral view. **D** Ovipositor and ovipositor sheath. **E** Hind leg.

reach 1cu-a; vein 2-Rs $2.9\times$ as long as vein r-rs; vein r-rs ends middle part of pterostigma behind the level of apex of pterostigma; vein Rs + M and 1Cu non-parallel; vein 1Cu with spiny setae basally. vein 2Rs+M extremely elongated, $0.4\times$ as long as vein 2-Rs and $1.05\times$ as long as 1-Rs, the origin of veins 2-Rs and apical abscissa of vein M non-connected; vein $2Cu_a$ nebulous apically with $2Cu_b$ completely absent. — *Legs*: Fore and mid legs with their femur and tibia flattened and expanded. Hind coxa rather robust, mostly shiny with distinct lateral groove; hind femur coriaceous, extremely robust with its median part distinct swollen as nearly oval shaped. Hind femur

dentigerous, with 2 large teeth and 10 medium sized teeth (4 of them between large teeth and 6 behind the apical large teeth); hind tibia elongate and $1.2\times$ longer than hind femur, with its basal narrow part $1.1\times$ as long as apical widened part (apical widened part rather extended with its maximum width $5.0\times$ as wide as minimum width of basal narrow part), inner side of widened part basally with two shallowly concave; hind tarsus with five tarsomeres; basitarsus $5.8\times$ as long as wide. — *Metasoma*: Metasoma with eight segments. First tergum and sternum not fused laterally, Tergite I rather slender, $1.2\times$ as long as tergite II. Pygidial impression reverse

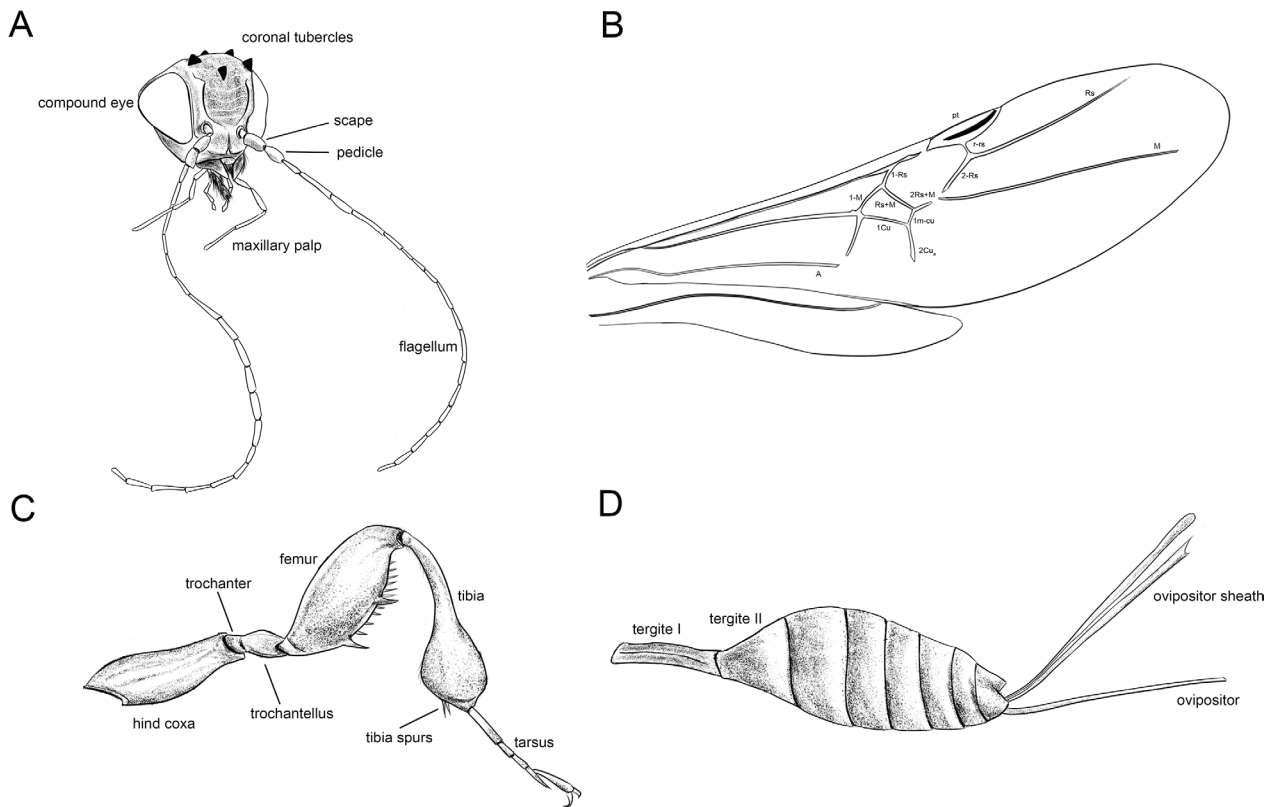


Figure 9. Details of *Tumidistephanus prometheus* Ge and Tan, sp. nov. Holotype ♀. **A** Head, frontal view. **B** Wings. **C** Hind leg. **D** Metasoma.

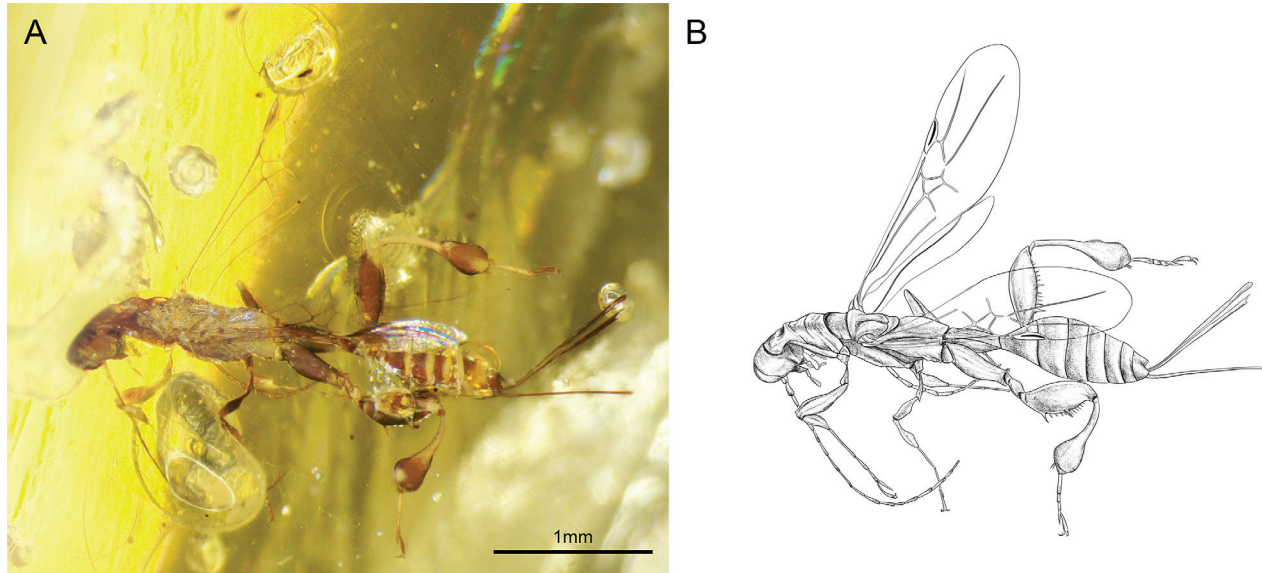


Figure 10. Habitus of Holotype ♀. *Tumidistephanus prometheus* Ge and Tan, sp. nov. **A** Photo of specimen. **B** Line drawing of habitus.

V-shaped. Ovipositor sheath 0.76× as long as metasoma. Ovipositor tip laterally compressed, apical without distinct teeth.

Remarks. This new species exhibits distinctive morphological features, such as the flattened and expanded femur and tibia of the fore and mid legs. This feature suggests that the subgenual organ of Stephanidae likely developed during the Cretaceous. Additionally, the new species has

a flattened and elliptical head, which is rarely found in extant species but reminiscent of the head shape of *Lagenostephanus*. A similar counterpart to its extremely swollen tibia can be found in the extant genus *Madegafoenus*; however, the swollen and multituberculate hind femur may be considered an autapomorphy. Combining these characteristics along with the results of the phylogenetic analysis, we assigned the new species and genus to the subfamily Lagenostephaninae Ge and Tan, **subf. nov.**

Genus †*Neurastephanus* Ge and Tan, gen. nov.

<https://zoobank.org/C615D4C7-32FB-442B-9F6A-38654EE7DC8E>

Type species. †*Electrostephanus neovenatus* Aguiar and Janzen, 1999.

Etymology. From “neura” (Latin for “vein”) and the generic name, *Stephanus* Jurine. The name refers to the peculiar venation of the type specimen. The gender of the name is masculine.

Diagnosis. Pronotum elongated, transversely rugose dorsally. Pronotal fold weakly developed with neck differentiated. Hind coxa strong, spindle shaped with its largely part smooth and shiny without transversely striate. Hind tibia with its median part moderately depressed. Hind tarsi 5-segmented. Forewing with vein 1-Rs shorter than 1-M; vein 2Rs+M distinct and elongate, non-connecting to 2-Rs and apical abscissa of vein M. Pterostigma comparatively wide, obtuse apically; vein 2Cu_b absent; vein A incomplete, only up to 1cu-a. Tergite I with tergum I and sternum I not fused, about 0.9 x as long as tergite II.

Remarks. Being a complex taxon that encompasses most Eocene crown wasps, the genus †*Electrostephanus*, presents challenges regarding its monophyly. van Achterberg (2002) claimed that the genus “is difficult to characterize and is mixed. Some species of the genus †*Electrostephanus* may belong to the subfamily Stephaninae.” Engel and Grimaldi (2004) separated the genus †*Denaestephanus* from †*Electrostephanus* but Engel and Ortega-Blanco (2008) indicated that the remaining †*Electrostephanus* species are still heterogeneous in lineages, with †*E. neovenatus* being enigmatic. We found that the species †*E. neovenatus* (Aguiar and Janzen, 1999) differed distinctly from all its congeners. Phylogenetic analysis indicated that it is reasonable to include this species in a new genus †*Neurastephanus* Ge and Tan, **gen. nov.** under the subfamily †Lagenostephaninae Ge and Tan, **subf. nov.** with only its type species †*N. neovenatus* (Aguiar and Janzen, 1999) **comb. nov.**

Subfamily Stephaninae Leach, 1815

= †Electrostephaninae Engel, 2005; Type genus: †*Electrostephanus* Brues, 1933

Genus †*Electrostephanus* Brues, 1933

Type species. †*Electrostephanus brevicornis* Brues, 1933.

Diagnosis. Hind coxa without dorsal tooth; metafemur bidentate or tridentate; hind tarsus of female with five tarsomeres; Forewing with vein 1-M arched, and distinctly longer than 1m-cu; veins Rs+M and 1Cu parallel; vein 1Cu

with spiny setae basally; vein 2Rs+M short, with slightly incisions between 2-RS and apical abscissa of vein M; 2Cu_a and 2Cu_b mostly present and tubular; hind wing with all veins absent except Sc+R present. Tergite I with tergum I and sternum I not fused. Tergite I nearly as long as Tergite II. Ovipositor sheath about as long as body length.

†*Electrostephanus brevicornis* Brues, 1933

Figures 11–13

†*Electrostephanus brevicornis* Brues, 1933:14 [holotype male, deposited in Königsberg Collection and presumed to be destroyed]; Aguiar and Janzen, 1999: 444–451 [keyed and discussed]; van Achterberg, 2002:11 [mentioned]; Aguiar, 2004:14 [catalog]; Engel, 2005:320 [discussed]; Engel and Ortega-Blanco, 2008:62 [keyed]; Li et al., (2017):196 [listed].

Type material. Neotype (designated here) ♀; BFU, Baltic amber; Eocene. Labeled as “Neotype: †*Electrostephanus brevicornis* Brues designator: Ge and Tan.” Part of the Si-Xun Ge collection.

Diagnosis. Forewing with vein R and vein A with setae at least along basal half of their length; vein r-rs distinctly shorter than 2-Rs (Fig. 12B); vein 2-Rs with its sub-median part slightly angled; vein 2Rs+M extremely short, slightly incision at the origin of veins 2-Rs and apical abscissa of vein M; vein 2Cu_b present. Metasoma tergum I and sternum I not fused (Fig. 11C; Fig. 12C). Tergite I about as long as Tergite II. Hind coxa strong, largely smooth and spindle shaped without striate. Hind femur tridentate; hind tarsus with five tarsomeres.

Description. Female. Total body length (from head anterior to metasoma distal margin, without ovipositor sheath) 6.5 mm; forewing length 4.3 mm; remaining part of ovipositor sheath 2.9mm. — *Head:* Antenna with 21 flagellomeres; the first flagellomere short and robust, and second flagellomere slender; Head globular, with compound eyes occupying about half portion of lateral surface; vertex with five tubercles; temple slightly bulging, smooth and shiny; occipital carina distinctly developed but not connected to hypostomal carina; hypostomal carina large. Maxillary palpus 5-segmented, elongate, elbowed between MP II (the second maxillary palpomere) and MP III. — *Mesosoma:* Pronotum robust with neck distinctly differentiated; neck at almost same level than middle part of pronotum postero-dorsally; middle and posterior part of pronotum with transverse carinae (as laterally) and with distinct oblique lateral groove; middle part of pronotum weakly differentiated from posterior part; posterior part of pronotum and mesonotum with sparse setosity; propleuron coriaceous; scutellum invisible. — *Wings:* Forewing with vein 1-M distinctly curved, 2.5× as long as vein 1-Rs and 1.3× vein 1m-cu; vein R with setae along all its length, while vein A only on the basal half; Four short, erect, equidistant spiny setae distinctly developed on the basal

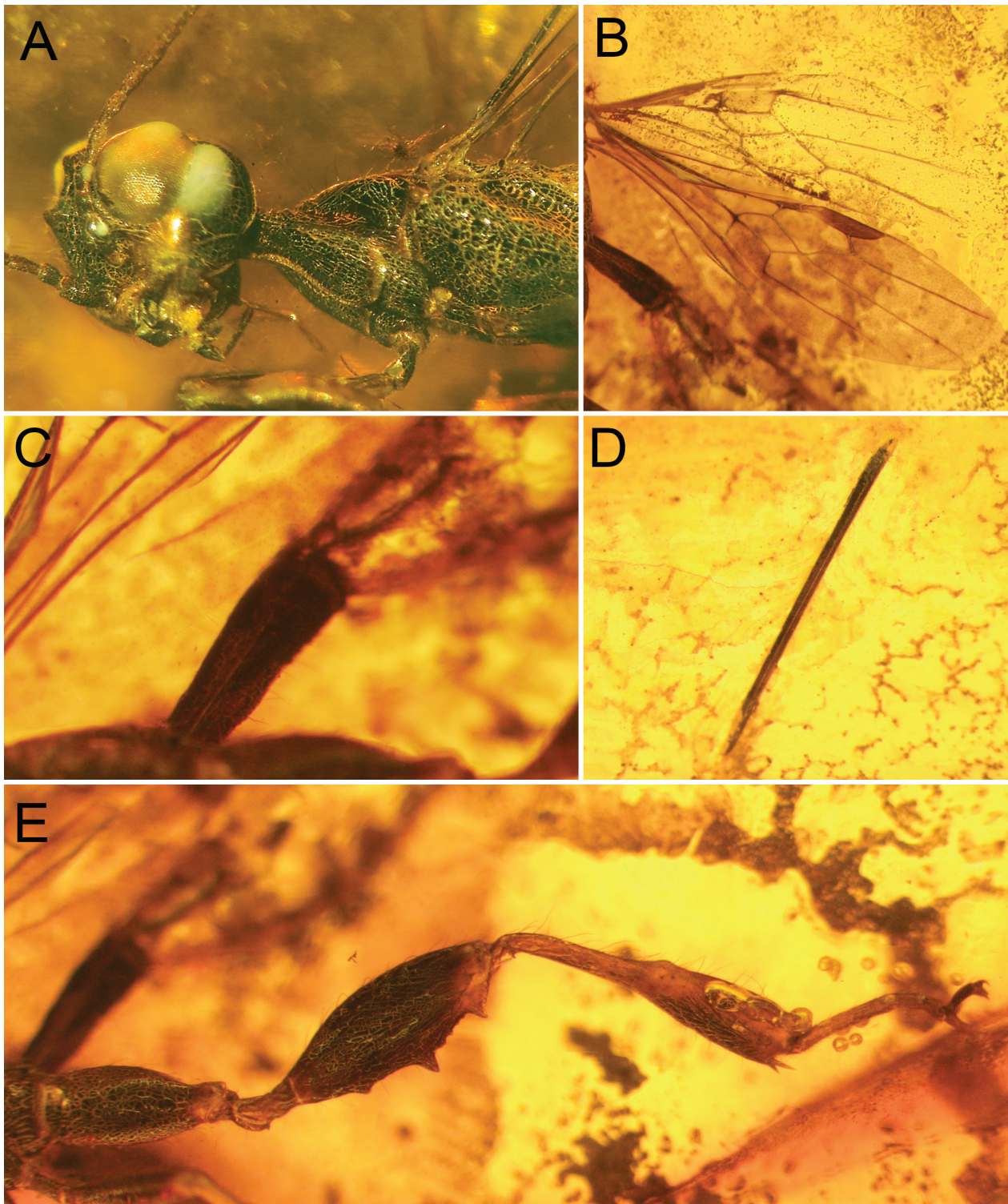


Figure 11. *Electrostephanus brevicornis* Brues, 1933. Neotype ♀. **A** Head and mesosoma, anterior-oblique view. **B** Wings. **C** Tergite I. **D** Ovipositor sheath. **E** Hind leg.

part of vein 1Cu; vein 2-Rs 2.2× as long as vein r-rs; vein r-rs ends inner side of pterostigma behind the level of apex of pterostigma; parastigmal vein (pv) elongated, ca 0.3× as long as pterostigma; vein 2-Rs with its sub-median part slightly upcurve angled; vein 2Rs+M extremely short 0.2× as long as vein 2-Rs, slightly incision at the origin of veins 2-Rs and apical abscissa of vein M; vein 2Cu_a distinct and curved apically with 2Cu_b distinctly developed. — *Legs*: Hind coxa robust,

smooth and shiny, spindle shaped without transversely striate; hind femur coriaceous, fusiform with its widest part near mid-point; ventral surface of hind femur with its basal tooth relatively small and blunt, a more acute triangular tooth developed near mid-length, and a widest tooth at the distal part; ca. four minor teeth or protuberances between medial tooth and distal tooth; hind tibia elongate and 1.1× longer than hind femur, with its basal narrow part 1.15× as long as apical widened part, inner

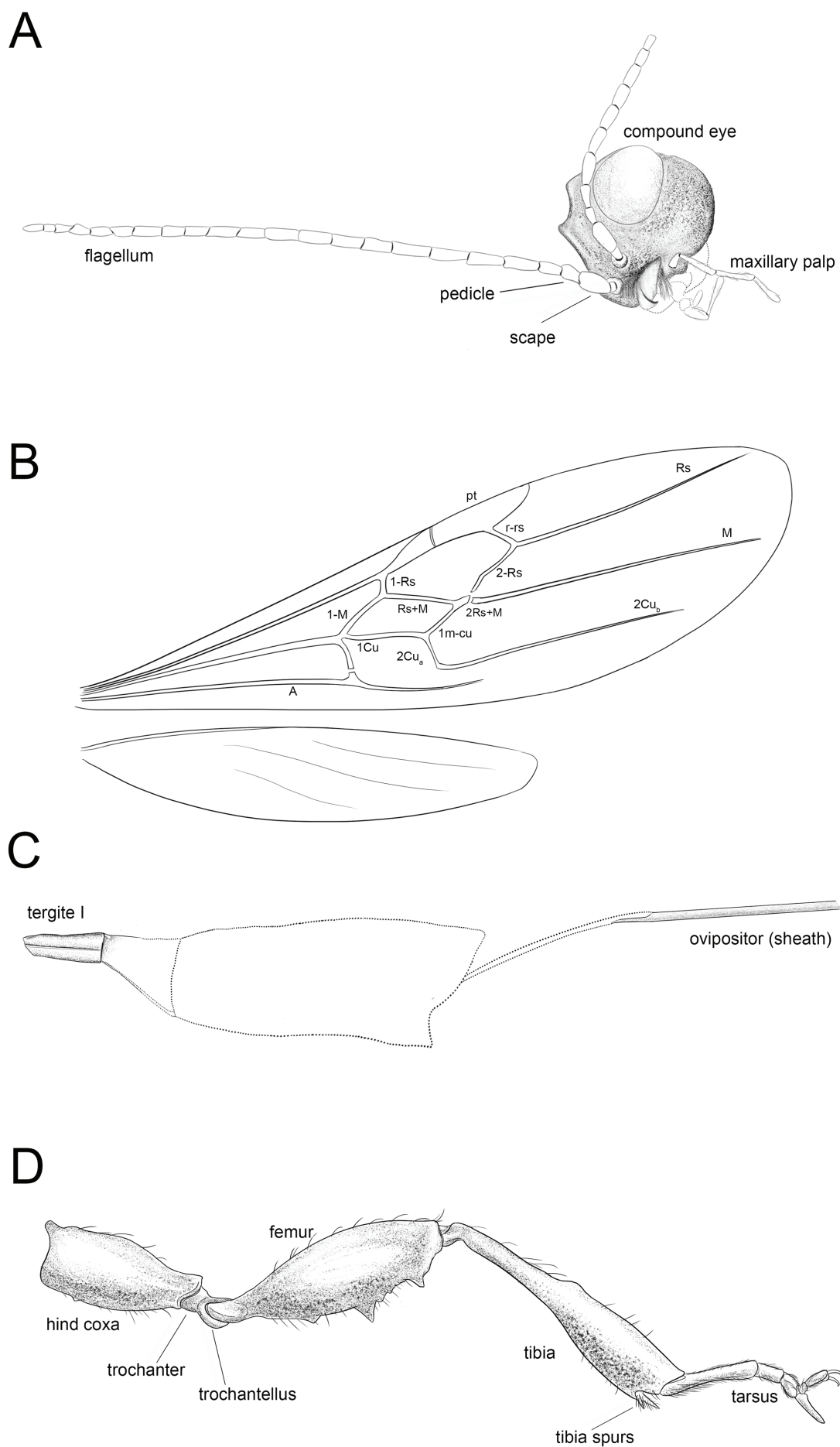


Figure 12. Details of *Electrostephanus brevicornis* Brues, 1933. Neotype ♀. **A** Head, anterior-oblique view. **B** Wings. **C** Metasoma as preserved. **D** Hind leg.

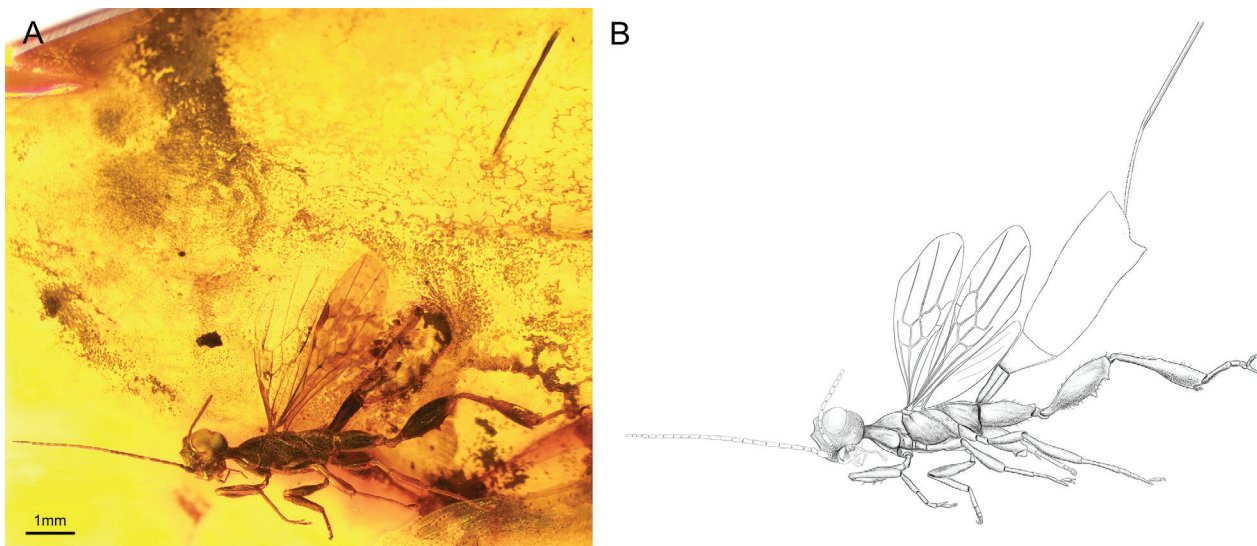


Figure 13. Habitus of neotype ♀. *Electrostephanus brevicornis* Brues, 1933. **A** Photo of specimen. **B** Line drawing of habitus.

side of widened part basally shallowly depressed; hind tarsus with five tarsomeres; basitarsus $6.4\times$ as long as wide. — *Metasoma*: Tergite I finely imbricate, $2.7\times$ as long as its widest part, with tergum I and sternum I not fused; tergite I at least $1.2\times$ as long as tergite II. Remainder of metasoma largely not preserved; pygidial area distinctly protruding apically. Basal half of ovipositor sheath missing, remaining parts of ovipositor sheath ca $0.9\times$ as long as metasoma. Ovipositor tip laterally compressed, without distinct teeth apically.

Remarks. The holotype of †*Electrostephanus brevicornis* Brues, 1933, has been lost (Aguiar and Janzen 1999; Engel 2008). Since there are few figures for this species to date, the only basis of species designation is the original description by Brues (1933). Our neotype fits well with the original description except for a few characteristics as follows: 1) in the original description of Brues (1933), the vein $2Rs+M$ ($= Rs+M_b$) is absent and there is no incision at the origin of vein $2+3Rs$ ($= 2-Rs$) and/or $2+3M$ ($= M$), while in the neotype, an extremely short vein $2Rs+M$ ($= Rs+M_b$) and slight incision between the origin of veins $2-Rs$ and apical abscissa of vein M ; 2) in the original description, the veins $2Cu_a$ and $2Cu_b$ are absent while in the neotype they are distinctly developed. However, we noticed that researchers may differ in describing the same characteristic. For instance, when the vein $2Rs+M$ ($= Rs+M_b$) is relatively short, it has often been considered absent, even in the original description of †*Protostephanus ashmeadi* Cockerell, 1906. Aguiar and Janzen (1999) pointed out that Brues did not regularly differentiate between nebulous and tubular veins, and merely chose to indicate their presence or absence. Furthermore, there were inevitably few morphological differences between the sexes (the holotype was male and the neotype is female). The missing type specimen and superficial original description greatly impede the understanding of the phylogeny of Stephanidae. Therefore, we ignore the subtle differences and designate this female as neotype of †*E. brevicornis* (Brues, 1933).

Genus †*Denaestephanus* Engel and Grimaldi, 2004

Type species. †*Electrostephanus sulcatus* Aguiar and Janzen, 1999.

Diagnosis. Tergite I with tergum I and sternum I fused, distinctly longer than tergite II. Forewing with free abscissa of vein M curved, distinctly longer than $1m-cu$; vein $2Rs+M$ absent or extremely short; vein $2Cu_a$ and $2Cu_b$ nebulous. Hind coxa smooth and without dorsal tooth; metafemur bidentate or tridentate; hind tarsus of female with five tarsomeres. Ovipositor about as long as body length.

†*Denaestephanus chaofeng* sp. nov.

<https://zoobank.org/DAE7AF65-E94B-40C7-9793-EE12F48F43D5>

Figures 14, 15

Holotype. ♀; BFU, Baltic amber, Eocene. Part of Si-Xun Ge's collection

Etymology. The new species was named after the third son of the Loong in Chinese mythology as the third species of †*Denaestephanus*.

Diagnosis. Pronotum comparatively robust, neck without distinct pronotal fold; anterior, middle and posterior part of pronotum almost at the same level in lateral view; mesonotum at the same level of pronotum; forewing with vein $1-M$ arched; vein $2Rs+M$ extremely short; vein $2Cu_a$ and $2Cu_b$ nebulous; hind femur relatively slender (Fig. 15D), minor teeth between basal and distal large tooth rather weakly developed; tergum I and sternum I fused (Fig. 14C; Fig. 15C), tergite I elongated as about $0.5\times$ as long as remainder of metasoma.

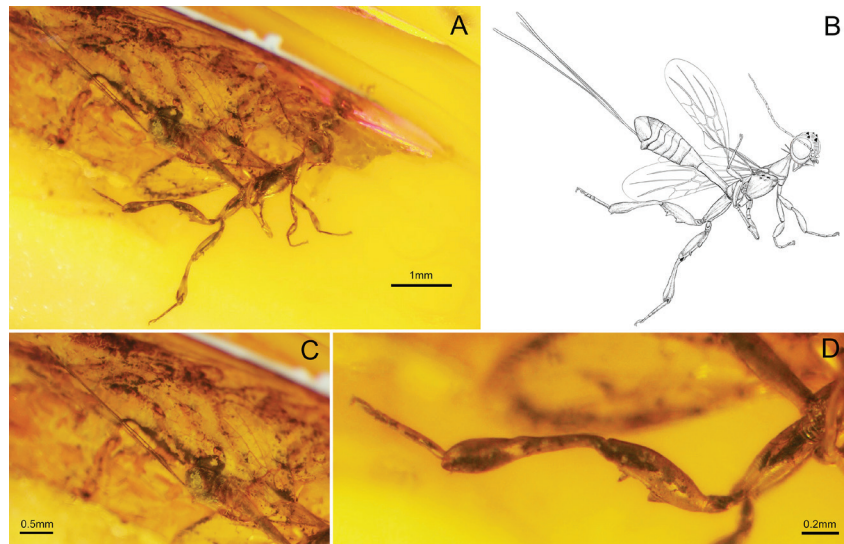


Figure 14. *Denaestephanus chaofeng* Ge and Tan, sp. nov. Holotype ♀. **A** Photo of specimen. **B** Line drawing of habitus. **C** Metasoma, lateral view. **D** Hind leg.

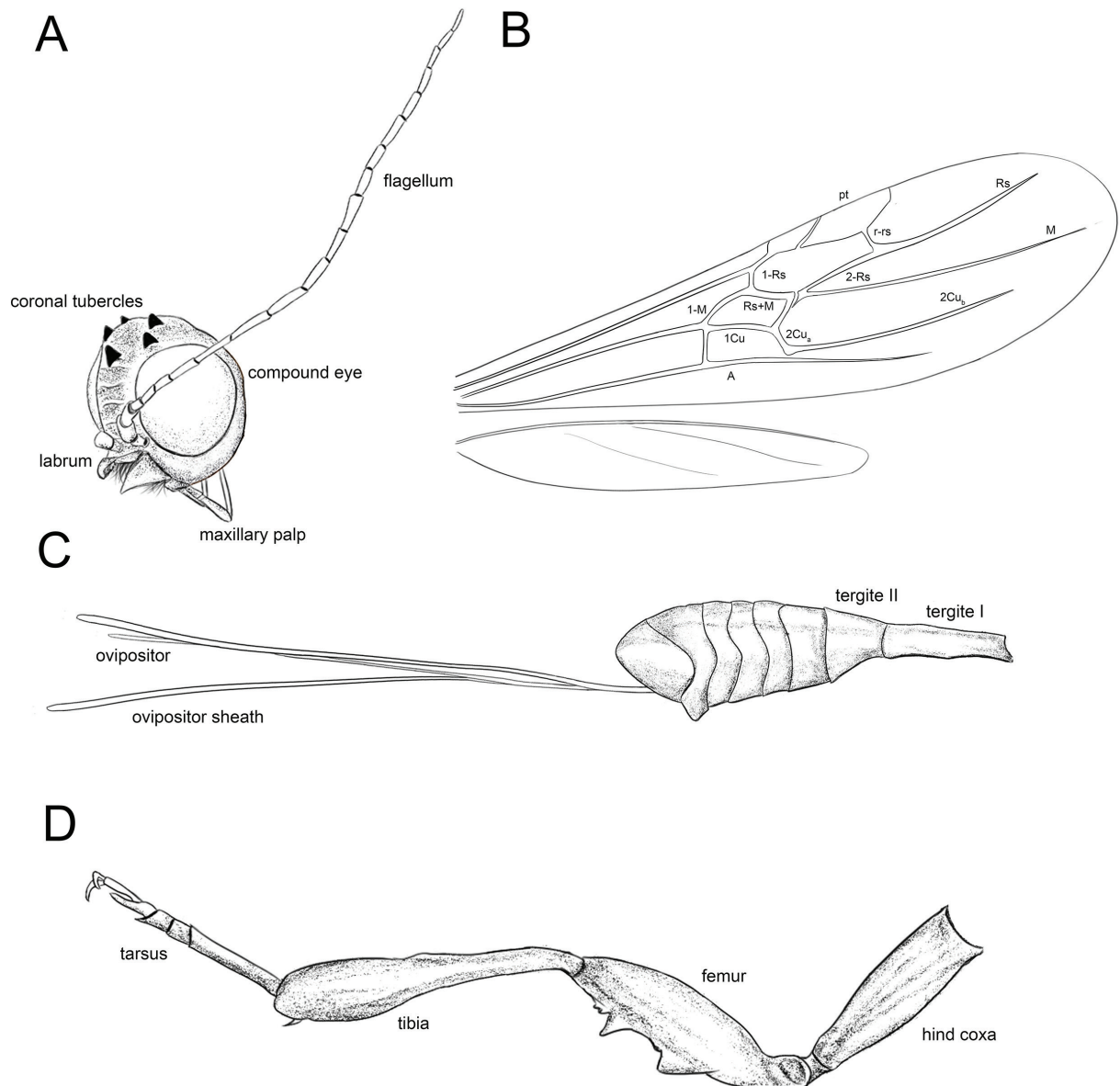


Figure 15. Details of *Denaestephanus chaofeng* Ge and Tan, sp. nov. Holotype ♀. **A** Head, frontal-oblique view. **B** Wings. **C** Metasoma. **D** Hind leg.

Description. Description: Female. Total body length (without ovipositor sheath) 3.6 mm; forewing length ca. 2.4 mm; ovipositor sheath 2.9 mm. — *Head*: Antenna with 19 flagellomeres; the first flagellomere short and robust while the second is elongated and slender; Head sub-globular (probably more or less traverse in dorsal view), with compound eyes occupying most part of lateral surface; vertex with five acute and triangular tubercles; temple comparatively flat, coriaceous; occipital carina distinctly developed and connected to hypostomal flange; hypostomal flange strong, without distinct rugae. Maxillary palpus 5-segmented, elbowed between MP II (maxillary palpomere II) and MP III; MP I and MP II distinctly short and strong, MP III–V long and slender; MP III slightly less than twice length of MP IV and MP V. — *Mesosoma*: Pronotum robust; neck without distinct pronotal fold; neck at almost same level of middle part of pronotum postero-dorsally; middle and posterior part of pronotum coriaceous, with slightly transverse carinae; middle part of pronotum not distinctly differentiated from posterior part; mesonotum at the same level of pronotum, without setosity; propleuron and mesopleuron coriaceous or imbricate; propodeum with its lateral view micro-sculptured; scutellum invisible. — *Wings*: Forewing with vein 1-M distinctly curved, 2.9× as long as vein 1-Rs and 1.7× vein 1m-cu; vein 2-Rs long, ca. 3.8× as long as vein r-rs; vein r-rs ends inner side of pterostigma behind the level of apex of pterostigma; parastigmal vein (pv) ca 0.4× as long as pterostigma; vein 2Rs+M (= Rs+M_b) extremely short, with its apical slightly incision at the origin of veins 2-Rs and apical abscissa of vein M; vein 2Cu_a and 2Cu_b nebulous. — *Legs*: Hind coxa comparatively slender, coriaceous, spindle shaped without transversely striate; hind femur coriaceous, relatively slender; ventral surface of hind femur bidentate, with its widest tooth developed at near 0.35× as its basal part; a more acute triangular tooth developed near 0.3× as its distal part with two small teeth behind, only one minor tooth weakly developed behind the basal large tooth; hind tibia about 1.2× as long as hind femur, with its basal narrow part as equal length as apical widened part, inner side of widened part basally moderately depressed; hind tarsus with five tarsomeres; basitarsus rather elongate, slightly longer than the length of all other tarsomeres. — *Metasoma*: Tergite I elongated and about 0.5× as long as the remainder of metasoma; tergite I with its ventral length 3.0× its maximum width; pygidial area not protruding apically; ovipositor sheath ca 0.8× as long as total body length and 1.2× as long as forewing length. Ovipositor tip laterally compressed, without distinct teeth apically.

Remarks. Two †*Denaestephanus* species, †*D. sulcatus* (Aguiar and Jazen, 1999) and †*D. tridentatus* (Brues, 1933), have been recognized before and only males have been described. This is also the first discovery of a female belonging to the genus, and thus we could supplement key characteristics of †*Denaestephanus* in phylogenetic research, such as the 5-segmented hind tarsus. Obviously, the single voucher specimen corrected the speculation of the 3-segmented hind tarsus by van Achterberg (2002). According to our phylogenetic analysis, †*Denaestepha-*

nus belongs to the subfamily Stephaninae and is a sister to all extant genera of the subfamily.

Genera *Incertae sedis*

Genus †*Tichostephanus* Engel, 2019

Type species. †*Tichostephanus hui* Engel, 2019

Diagnosis. Male, antenna relatively short with 12 robust flagellomeres. Head globose with about seven distinct coronal teeth on upper frons and vertex around ocelli; veins of forewing strongly reduced; pterostigma sub-parallel-sided, distinct elongate and acute apically; vein 1Rs/1M straight, few veins indistinguishable; vein Rs+M absent, vein 2Rs+M and 1m-cu continuous, forming straight elongated vein between anterior apex of subdiscal cell to origin of 2-Rs, thus forming massive submarginal cell owing to merging of submarginal and discal cells; apical abscissa of vein M absent; vein 2Cu_b absent, vein A elongated beyond 1cu-a and almost reach 2Cu_a; Hind wing with cu-a absent. Hind femur slender, edentulous. Hind tibia with its basal part petiolate while apical half distinctly flattened, without depression at inner side.

Remarks. In our phylogenetic analysis, the monotypic genus †*Tichostephanus* showed a unique lineage that was sister to all other Stephanidae species. †*Tichostephanus* has many peculiar characteristics, like a short and robust antenna, absence of vein Rs+M, massive submarginal cell, edentulous hind femur, and strongly extended metasomal apex, which is not found in all other Stephaninae or even Stephanidae species. Combined with the phylogenetic analysis results, †*Tichostephanus* is excluded from Stephaninae. Considering that the known specimen is male (lacking many important morphological information of females in phylogeny) and only contain one species in its lineage, we prudently treated †*Tichostephanus* as *incertae sedis* within the family.

Genus †*Phoriostephanus* Engel and Huang, 2016

Type species. †*Phoriostephanus exilis* Engel and Huang, 2016.

Diagnosis. Head globose, ocelli gathered closely on vertex. Front tibia with distinct dentition and not compressed medially. Pronotum elongated with neck differentiated. Forewing with vein 2Rs+M distinctly developed, about as long as vein Rs+M. Hind femur comparatively slender, edentulous. Hind tibia slender, without concavity medially.

Remarks. In the original description by Engel and Huang (2016), the monotypic genus †*Phoriostephanus* was assigned to the subfamily Schlettereriinae, as the type spe-

cies with a mediodorsal swelling on its hind coxa, as well as a non-petiolate hind tibia. However, according to the type specimen, it also showed many unique characteristics that separate it from all known Stephanidae (e.g., a globose head without tubercles on the vertex, an edentulous hind femur, and a venation with the discal cell I distinctly shorter than sub-discal cell I). Notably, Engel and Huang (2016) also thought that †*P. exilis* stands out disparately among Stephanoidea. It may represent a more basal lineage sister to Schlettereriinae or may even be given family rank and placed as sister to Stephanidae. Based on the results of our phylogenetic analysis, †*Phoristephanus* is excluded from Schlettereriinae. Considering that the known specimen is male (lacking many important morphological information of females in phylogeny) and only contain one species in its lineage, we prudently treated Schlettereriinae as *incertae sedis* within the family.

Genus †*Aphanostephanus* Ge and Tan, gen. nov.

<https://zoobank.org/10114E82-8813-4751-8F3B-98F4B5B-D1E79>

Type species. †*Electrostephanus janzeni* Engel, 2005.

Diagnosis. Head globose, compound eyes comparatively small, occupying less than half portion of lateral

surface. Pronotum elongated with neck differentiated. Forewing with vein 2Rs+M rather short, directly connecting to veins 2-Rs and apical abscissa of vein M without incisions; vein 2Cu_a pigmented and vein 2Cu_b absent. Metasoma with tergum I and sternum I not fused laterally, tergite I short and robust, about as long as tergite II. Ovipositor almost as long as body length.

Etymology. From “Aphanes” (Greek for “vague”) and the generic name *Stephanus* Jurine. The name refers to the puzzling position of the genus within a family. The gender of the name is masculine.

Remarks. In the original description by Engel (2005), the type species was indicated to be similar to †*Neurastephanus neovenatus* **comb. nov.** which is a species here considered to belong to †Lagenostephaninae **subf. nov.** However, it differs from †*N. neovenatus* in having vein 1-M straight; vein 2Rs + M short, directly connected to vein 2-Rs, and the apical abscissa of vein M. In addition, the paratype female also showed its ovipositor sheath about as long as the body length (in †Lagenostephaninae as long as the metasoma). Combining our phylogenetic results, this taxa showed its lineage sister to †Lagenostephaninae + Schlettereriinae, however, there is no synapomorphies or characteristics with significant evolutionary significance that can define it as a distinct group; thus, we prudently treated the genus as *incertae sedis* in the Stephanidae.

3.4. Key to the extinct and extant genera of the family Stephanidae

- 1 Vertex without distinct tubercles; front tibia with distinct dentition and not compressed medially †*Phoristephanus* Engel and Huang, 2016
- 1' Vertex with tubercles; front tibia compressed medially 2
- 2 Hind femur smooth and tubular, without dentation; antenna with 12 flagellomeres; flagellomeres robust and short †*Tichostephanus* Engel, 2019
- 2' Hind femur robust and with dentation; antenna with more than 12 flagellomeres; flagellomere comparatively long and slender 3
- 3 Hind coxa with small dorsal tooth; hindwing with vein 1cu-a present; metasoma with tergum I and sternum I distinctly separated laterally; (subfamily Schlettereriinae Orfila) 4
- 3' Hind coxa without dorsal tooth; hindwing with vein 1cu-a absent; metasoma with tergum I and sternum I variable 6
- 4 Vertex with 7 teeth-shaped tubercles; vein 2Cu_b of fore wing absent †*Kronostephanus* Engel and Grimaldi, 2013
- 4' Vertex with 3–5 teeth-shaped tubercles; vein 2Cu_b of fore wing present 5
- 5 Vein 1-Rs of forewing as long as 1-M; [New Jersey amber] †*Archaeostephanus* Engel and Grimaldi, 2004
- 5' Vein 1-Rs of forewing distinctly shorter than vein 1-M *Schlettererius* Ashmead, 1900
- 6 Forewing with vein 2Rs+M rather short, directly connected to veins 2-Rs and apical abscissa of vein M without incisions; ovipositor sheath about as long as body length †*Aphanostephanus* Ge and Tan, gen. nov.
- 6' Forewing with vein 2Rs+M differentiated, at least with incisions with free abscissa of vein M and vein 2-Rs; length of ovipositor sheath variable 7
- 7 Vein 2Rs + M differentiated, with distinct space between free abscissa of vein M and vein 2-Rs; vein r-rs of forewing about as long as vein 1-Rs; vein Rs+M of fore wing converging to vein 1Cu distally; ovipositor sheath about as long as metasoma; (subfamily †Lagenostephaninae Ge and Tan, **subf. nov.**) 8
- 7' Forewing with vein 2Rs + M with incisions between free abscissa of vein M and vein 2-Rs; vein r-rs longer than 1-Rs; veins Rs+M and 1Cu of fore wing parallel; ovipositor sheath about as long as body length; (subfamily Stephaninae Leach) 10

- 8 Metasoma with tergum I and sternum I fused; pronotum extremely elongated, nearly tape-shaped; neck without pronotal fold; hind coxa tube-shaped; [Myanmar amber] †*Lagenostephanus* Li, Rasnitsyn, Shih and Ren
- 8' Metasoma with tergum I and sternum I separated; pronotum relatively elongate; neck with distinct pronotal fold; hind coxa strong, spindle-shaped 9
- 9 Apical half of hind tibia strongly dilated, almost as wide as hind femur; [Myanmar amber] †*Tumidistephanus* Ge and Tan, gen. nov.
- 9' Apical half of hind tibia relatively slender, distinctly narrower than hind femur; [Baltic amber] †*Neurastephanus* Ge and Tan, gen. nov.
- 10 Metasoma with tergum I and sternum I separated; [Baltic amber] †*Electrostephanus* Brues
- 10' Metasoma with tergum I and sternum I fused 11
- 11 Hind coxa smooth; without rugose or carina; [Baltic amber] †*Denaestephanus* Engel and Grimaldi
- 11' Hind coxa with distinct transverse costae or striae 12
- 12 Apical half of hind tibia without distinct expansion; hind tarsus of female 5-segmented *Stephanus* Jurine, 1801
- 12' Apical half of hind tibia distinctly wider than its basal half; hind tarsus of female 3-segmented 13
- 13 First metasomal tergite short, nearly as long as tergite II †*Protostephanus* Cockerell, 1906
- 13' First metasomal tergite rather elongated, distinctly longer than tergite II 14
- 14 Hind coxa robust and spindle shaped; hind femur largely smooth; (tribe Megischini Engel and Grimaldi) 15
- 14' Hind coxa slender, rather elongated and tube-shaped; hind femur largely coriaceous; (tribe Foenatopodini Enderlein) 18
- 15 Vein 1-Rs of forewing weakly curved and long; hindwing with vein M+Cu at least partly sclerotized; pronotum with sub-medial transverse protuberance *Afromegischus* van Achterberg, 2002
- 15' Vein 1-Rs of fore wing straight and usually short; hindwing with vein M+Cu absent or only pigmented; pronotum without sub-medial transverse protuberance 16
- 16 Temple with pale yellowish streak behind eye; ovipositor sheath without ivory subapical band *Pseudomegischus* van Achterberg, 2002
- 16' Temple without pale yellowish streak behind eye; ovipositor with ivory subapical band 17
- 17 Apical spiny seta on vein M+Cu of fore wing present near vein 1-M; vein 2-1A of fore wing distinctly developed *Megischus* Brullé, 1846
- 17' Apical spiny seta on vein M+Cu of fore wing absent near vein 1-M; vein 2-1A of fore wing completely absent *Hemistephanus* Enderlein, 1906
- 18 Venation of fore wing strongly reduced and veins Rs+M and 1m-cu entirely absent 19
- 18' Venation of fore wing almost complete and veins Rs+M and 1m-cu present, at least pigmented 20
- 19 Apical half of hind tibia strongly inflated, 2.8–3.7 times wider than basal narrow part, almost as wide as hind femur *Madegafoenus* Benoit, 1951
- 19' Apical half of hind tibia` at most moderately inflated, less than 2.5 times wider than basal narrow part *Foenatopus* Smith, 1860
- 20 Median groove of vertex more or less developed; vein 2-1A of forewing basally shortly sclerotized and distinctly pigmented extends beyond vein 1cu-a; inner side of narrowed part of hind tibia granulate *Profoenatopus* van Achterberg, 2002
- 20' Median groove of vertex absent; vein 2-1A of forewing absent or nearly so; inner side of narrowed part of hind tibia smooth or punctate *Parastephanellus* Enderlein, 1906

4. Discussion

4.1. Phylogeny of Stephanidae

Prior to this work, only van Achterberg (2002) and Li et al (2017) had explored the intergeneric phylogenetic relationships within the family. However, both studies employed a limited number of characters (22 in van Achterberg (2002) and 34 in Li et al. (2017)), and some of these characters had notable flaws in their construction and selection. Another problem shown in previous studies was that both of them chose the “genus” as the smallest taxonomic unit in their phylogenetic analyses, which not only resulted in insufficient consideration of the enormous morphological diversity within a genus, but also

undermines the phylogeny results when there is problematic genus (*i.e.* the polyphyletic †*Electrostephanus*). To address the above issues, in this study, we increased the number of selected morphological characters and chose species as the minimum taxonomic unit for phylogenetic analysis. Additionally, when including extinct genera, our analysis encompassed nearly all fossil specimens associated with the family known to date.

Prior to this study, Stephanidae was formerly divided into two major clades, namely Schlettereriinae and Stephaninae (van Achterberg, 2002; Li et al., 2017). By including the newly discovered specimens, our morphological phylogenetic analyses have proposed a new subfamily (*i.e.*, †Lagenostephaninae) that is sister to Schlettereriinae. To resolve the polyphyly of †*Electrostephanus*, the genus was redefined, retaining the type species †*E. brevicornis*

Table 1. Comparisons of some key morphological characteristics between subfamilies of Stephanidae.

Characters/subfamilies	†Lagenostephaninae	Schlettereriinae	Stephaninae
Anterior part of pronotum	Elongated as “neck”	Not elongated as “neck”	Elongated as “neck”
Hindwing with vein Cu-a	Absent	Present	Absent
Forewing with the junction of 2-Rs, M, and 2Rs+M	Distinctly separated	Distinctly separated	Variable
Hind coxa with surface sculpture	Largely smooth	Rugose	Variable
Hind coxa with dorsal teeth	Absent	Present	Absent
Hind tarsus of females	5-segmented	5-segmented	Variable
Metasoma with tergum I and sternum I	Variable	Separated	Variable
Length of ovipositor	Approximately as long as metasoma	Approximately as long as body	Approximately as long as body

and †*E. petiolatus*, and assigning the other two species to new genera †*Neurastephanus* and †*Aphanostephanus*. Based on our results, the redefined †*Electrostephanus* belongs to the subfamily Stephaninae, thus receiving support from the results of Li et al. (2017) and confirming the synonymy of *Electrostephaninae* with *Stephaninae*.

Within the extant groups of subfamily Stephaninae, most genera clustered into two major clades with the genus *Stephanus* as the most basal group, similar to the previous results of van Achterberg (2002), Engel and Grimaldi (2004), and Li et al. (2017). However, given our results, reclassification is necessary, as the genus *Afromegischus* should be moved from the tribe Foenatopodini to the tribe Megischini.

Notably, there are still a few taxa with undecided positions in the current phylogenetic hypothesis. †*Tichostephanus* and †*Phoriostephanus* have shown their unique lineage successively sister to other Stephanidae and are considered as early disparate forms among Stephanoidea. The resolution of the taxonomic status of the above two taxa may depend on the discovery of female specimens. The newly established genus †*Aphanostephanus* has shown its lineage sister to †*Lagenostephaninae* + *Schlettereriinae* to be rather weakly supported, and it appears that the taxon sampling in the present study is insufficient to confidently assign its position, which requires further investigation.

4.2. Evolution of key morphological characteristics

Although it is a group with little-known life history, many characteristics of Stephanidae are related to its biology according to the available literature (Taylor, 1967; Vilhemsen 1997; van Achterberg, 2002). The modified pronotum may facilitate the head when the adult slants backward, and the compressed fore and hind tibia indicate subgenual organs that help detect the host. All of the above characteristics have been observed in both fossil and extant Stephanidae species (except for †*Phoriostephanus*, which may be considered one of the most basal groups or a sister group of the family), thus implying little variation in the biology and niche of these crown wasps since the Cretaceous. Another structure with important evolutionary significance is the “wasp waist,”

which provides maneuverability, flexibility, and posture for oviposition. In †*Tichostephanus*, the dorsal margin of the propodeum is arc-shaped in lateral view, while that in other Stephanidae is nearly straight. Li et al. (2015) indicated that this character reflects a transitional state of the evolution of the “wasp waist” from †*Ephialtitidae* to Stephanidae, reflecting the comparatively basal position of †*Tichostephanus* within Stephanidae.

Some synapomorphies have been observed only in extinct taxa. In the newly established subfamily †*Lagenostephaninae*, the ovipositor of †*Tumidistephanus*, and †*Lagenostephanus* is approximately as long as the metasoma. This character state may be of ecological significance, as the comparatively short ovipositors may not be enough to penetrate the xylem, and their comparatively small size (†*T. prometheus* may be the smallest known crown wasp with a total body length of 2.8 mm and ovipositor sheath of 1.05 mm) may enable them to complete development on some small-sized hosts (e.g. bark beetles), thus reflecting a diverse niche to extant stephanids that are parasitoids of xylem borers. The non-rugose metasoma tergite I and hind coxa are also only present in fossil taxa, implying that the rugose or carinate counterparts are developed parallel evolutionary in extant taxa, most likely to facilitate movements in narrow galleries. Intriguingly, almost all fossil Stephanids have shown metasomal tergite I about as long as tergite II; however, in the extant taxa the length of tergite I is somewhat variable even within a genus (i.e., rather short in *Schlettererius cinctipes* but longer in *S. determinatoris*). This may indicate that this elongation developed parallel in diverse lineages of Stephanidae as an adaptation to provide more physical strength for females allowing oviposition deeper in the wood.

Two key characteristics (i.e. metasoma with tergum I and sternum I fused or not; the number of hind tarsal segments of females) were considered as play important roles in generic identification. The former one could be observed as a variable in both Stephaninae and †*Lagenostephaninae* (but stable in *Schlettereriinae*, with tergum I and sternum I separated); and the later one is stable in both †*Lagenostephaninae* and *Schlettereriinae* (hind tarsal with 5 segments in females), but variable in Stephaninae. This indicates that these characteristics probably evolved parallel after the divergence of the two subfamilies. Particularly, within Stephaninae, the most basal genus †*Electrostephanus* with tergum I and sternum I separat-

Table 2. A list of extinct species of Stephanidae.

Taxa	Locality	Horizon	References
Family Stephanidae			
Subfamily Schlettereriinae Orfila			
Genus † <i>Archaeostephanus</i> Engel and Grimaldi			
† <i>Archaeostephanus corae</i> Engel and Grimaldi, 2004	New Jersey	Cretaceous	Engel and Grimaldi (2004)
Genus † <i>Kronostephanus</i> Engel and Grimaldi			
† <i>Kronostephanus zigrasi</i> Engel and Grimaldi, 2013	Myanmar	Cretaceous	Engel et al., (2013)
Subfamily † <i>Lagenostephaninae</i> Ge and Tan, subf. nov.			
Genus † <i>Lagenostephanus</i> Li, Rasnitsyn, Shih and Ren			
† <i>Lagenostephanus lii</i> Li, Rasnitsyn, Shih and Ren, 2017	Myanmar	Cretaceous	Li et al., (2017)
Genus † <i>Tumidistephanus</i> Ge and Tan, gen. nov.			
† <i>Tumidistephanus prometheus</i> Ge and Tan, sp. nov.	Myanmar	Cretaceous	This study
Genus † <i>Neurastephanus</i> Ge and Tan, gen. nov.			
† <i>Neurastephanus neovenatus</i> Aguiar and Janzen, (1999)	Baltic	Middle Eocene	Aguiar and Janzen (1999)
Subfamily Stephaninae Leach			
Genus † <i>Electrostephanus</i> Brues			
† <i>Electrostephanus brevicornis</i> Brues, 1933	Baltic	Middle Eocene	This study
† <i>Electrostephanus petiolatus</i> Brues, 1933	Baltic	Middle Eocene	Engel and Grimaldi (2004)
Genus † <i>Protostephanus</i> Cockerell			
† <i>Protostephanus ashmeadi</i> Cockerell, 1906	Florissant, Colorado	Late Eocene	Cockerell (1906)
Genus † <i>Denaestephanus</i> Engel and Grimaldi			
† <i>Denaestephanus sculcatus</i> (Aguiar and Janzen, 1999)	Baltic	Middle Eocene	Engel and Grimaldi (2004)
† <i>Denaestephanus tridentatus</i> (Brues, 1933)	Baltic	Middle Eocene	Engel and Grimaldi (2004)
† <i>Denaestephanus chaofeng</i> Ge and Tan, sp. nov.	Baltic	Middle Eocene	This study
<i>Incertae sedis</i>			
Genus † <i>Tichostephanus</i> Engel			
† <i>Tichostephanus hui</i> Engel, 2019	Myanmar	Cretaceous	Engel (2019)
Genus † <i>Phoriostephanus</i> Engel and Huang			
† <i>Phoriostephanus exilis</i> Engel and Huang, 2016	Myanmar	Cretaceous	Engel and Huang, (2016)
Genus † <i>Aphanostephanus</i> Ge and Tan, gen. nov.			
† <i>Aphanostephanus janzeni</i> (Engel, 2005)	Baltic	Middle Eocene	Engel (2005)

ed and 5-segmented hind tarsus in females. However, the position in the phylogenetic analysis of †*Protostephanus* which has a fused tergite I and 3-segmented hind tarsus as sister to †*Denaestephanus* (female with fused tergite I and 5-segmented hind tarsus) is weakly supported. The low support values of the topology and the repeated changes in the states of the hind tarsus may be caused by several missing characters in these fossil specimens, especially in the compression fossil †*Protostephanus*.

4.3. Clues on the origin of Stephanidae

To date, 14 species of extinct Stephanidae (Table 2) have been reported and represent all extant subfamilies as well as some early lineages. The comparatively high diversity of basal lineages implies that the diversification of Stephanidae occurred between the early and mid-Cretaceous. Based on our dating using the morphological clock, the origin of stem-Stephanidae is dated back to the Late Jurassic, which is much later than estimated by molecular clock based on genomic data: the divergence of Stephanoidea and Evanioidea was estimated to occur in the Late Triassic (Peters et al., 2017).

This difference may indicate limitations of our time tree and morphological clock in general. However, we took the risk of using this method for two reasons: (1) the molecular data is very limited for Stephanidae species, with less than half of the 10 extant genera sequenced and mostly only DNA barcodes available; (2) the known fossils of the Stephanidae do not exhibit dramatic morphological variation. Moreover, all known extant species of the Stephanidae are parasitoids of xylem borers with occasional host not representing major life style shifts. The only group for which a significant host shift may be expected, †*Lagenostephaninae* subf. nov., has become extinct.

Notably, two extinct early-branching of Stephanidae (*i.e.*, †*Tichostephanus* and †*Phoriostephanus*) occupy lineages that are clearly separated from the three principal branches of the family, with their roots likely dating back to the Late Jurassic or Early Cretaceous. The above-mentioned groups show relatively modern characteristics (both of them with wing venation rather reduced compared to the extant primitive Stephanidae *Schlettererius*), which indicates that these early Stephanoidea/Stephanidae had undergone a period of evolution as of the Jurassic period, which is consistent with the time of the large diversification of parasitoid wasps. Moreover, the “mod-

ern” fossil specimen status may hint on the presence of unrecognized “dark lineages” in fossil Stephanidae.

As a group with worldwide distribution and comparatively rare population, a classic problem with Stephanidae is the difficulty in obtaining molecular samples. So far, there is no molecular-based phylogenetic study on the family. Ideally, a holistic approach, where alternative types of data are used for extant and extinct taxa together, should be applied whenever possible. In the present case, a purely morphological dataset was the only practical approach to glimpse the phylogeny, as molecular data are not yet available for many genera of Stephanidae.

5. Author Contributions

Si-Xun Ge: Conceptualization (lead); data curation (lead); formal analysis (lead); methodology (equal); resources (lead); software (lead); visualization (supporting); writing original draft (lead).

Zhuo-Heng Jiang: formal analysis (equal); software (equal); visualization (lead). Li-Li Ren: funding acquisition (equal); project administration (equal); resources (equal); supervision (equal); validation (lead); visualization (equal); writing review and editing (supporting).

Jiang-Li Tan: conceptualization (equal); methodology (equal); supervision (lead); funding acquisition (lead); validation (equal); writing review and editing (lead).

Cornelis van Achterberg: methodology (equal); review and editing (equal).

6. Acknowledgements

We thank Mr. Hong-Yu Li (China Agricultural University, Beijing), Dr. Han Xu (Beijing Forestry University, Beijing), Dr. Xin-Yu Li (Beijing Forestry University, Beijing), Dr. Jia-Long Huang (College of Geography and Oceanography, Minjiang University, Fuzhou), Dr. Tao Li (General Station of Forest and Grassland Pest Management, National Forestry and Grassland Administration, Shenyang) and Prof. Shi-Xiang Zong, (Beijing Forestry University, Beijing) for their great support for this study. The research was jointly supported by the National Natural Science Foundation of China (NSFC, No. 31872263, 31201732, 31572300) and National Key R and D Program of China (2022YFD1401000).

7. References

- Aguiar AP, Janzen JW (1999) An overview of fossil Stephanidae (Hymenoptera), with description of two new taxa from Baltic amber, and key to species of *Electrostephanus* Brues. *Entomologica Scandinavica* 30: 443–452.
- Aguiar AP (2001) Revision of the Australian Stephanidae (Hymenoptera). *Invertebrate Taxonomy* 15: 763–822. <https://doi.org/10.1071/IT00006>
- Aguiar AP (2004) World catalog of the Stephanidae (Hymenoptera: Stephanioidea). *Zootaxa* 753: 1–120. <https://doi.org/10.11646/zootaxa.464.1.1>
- Aguiar AP (2006) The Stephanidae (Hymenoptera) of Mexico, with description of six new species and key to western *Foenatopus* Smith. *Zootaxa* 1186(1): 1–56. <https://doi.org/10.11646/zootaxa.1186.1.1>
- Aguiar AP, Jennings JT, Turrisi GF (2010) Three new Middle-Eastern species of *Foenatopus* Smith (Hymenoptera: Stephanidae) with a new host record and key to species with two spots on the metasoma. *Zootaxa* 2714(1): 40–58. <https://doi.org/10.11646/zootaxa.2714.1.2>
- Aguiar AP, Sharkov A (1997) Blue pan traps as a potential method for collecting Stephanidae (Hymenoptera). *Journal of Hymenoptera Research* 6(2): 422–423.
- Benoit PLG (1949) Les Stephanoidae (Hym.) du Congo belge. *Revue de zoologie et de botanique africaines* 42(3–4): 285–294.
- Binoy C, van Achterberg C, Girish Kumar P, Santhoshi S, Sheela S (2020) A review of Stephanidae (Hymenoptera: Stephanioidea) from India, with the description of five new species. *Zootaxa* 4838(1): 1–51. <https://doi.org/10.11646/zootaxa.4838.1.1>
- Branstetter MG, Danforth BN, Pitts JP, Faircloth BC, Ward PS, Buffington ML, Gates MW, Kula RR, Brady SG (2017) Phylogenomic insights into the evolution of stinging wasps and the origins of ants and bees. *Current Biology* 27: 1019–1025. <https://doi.org/10.1016/j.cub.2017.03.027>
- Brues CT (1933) The parasitic Hymenoptera of the Baltic amber. Part 1. *Bernstein Forschungen* 3: 4–178.
- Chao HF (1964) Description of new species of Stephanidae (Hymenoptera, Ichneumonoidea) from South China. *Acta entomologica Sinica* 13(3): 376–395. [in Chinese with English summary]
- Chen HY, van Achterberg C, Xu ZF (2016) Description of a new species of *Foenatopus* Smith from China and the male of *Parastephanus brevicoxalis* (Hymenoptera, Stephanidae). *ZooKeys* 612: 113–123. <https://doi.org/10.3897/zookeys.612.9781>
- Cockerell TDA (1906) Fossil Hymenoptera from Florissant, Colorado. *Bulletin of the Museum of Comparative Zoology* 50(2): 33–58.
- Engel MS, Grimaldi DA (2004) The first Mesozoic stephanid wasp (Hymenoptera: Stephanidae). *Journal of Paleontology* 78: 1192–1197.
- Engel MS, Huang DY (2016) A new crown wasp in Cretaceous amber from Myanmar (Hymenoptera: Stephanidae). *Creataceous Research* 69: 56–61. <https://doi.org/10.1016/j.cretres.2016.08.014>
- Engel MS, Ortega-Blanco J (2008) The fossil crown wasp *Electrostephanus petiolatus* Brues in Baltic Amber (Hymenoptera, Stephanidae) designation of a neotype, revised classification, and a key to amber Stephanidae. *Zookeys* 4: 55–64.
- Engel MS (2005) The crown wasp *Electrostephanus* (Hymenoptera: Stephanidae): discovery of the female and a new species. *Polskie Pismo Entomologiczne* 74(3): 317–332.
- Engel MS (2019) A new crown wasp in mid-Cretaceous amber from northern Myanmar (Hymenoptera: Stephanidae). *Palaeontology* 2(3): 229–235.
- Engel MS, Grimaldi DA, Ortega-Blanco J (2013) A stephanid wasp in mid-Cretaceous Burmese amber (Hymenoptera: Stephanidae), with comments on the antiquity of the hymenopteran radiation. *Journal of the Kansas Entomological Society* 86(3): 244–252. <https://doi.org/10.2317/JKES130206.1>
- Fabricius JC (1804) *Systema Piezatorum secundum ordines, genera, species, adjectis synonymis, locis, observationibus, descriptionibus*. Brunsvigae, Carolus Reichard, 439 pp.
- Ge SX, Ren LL, Tan JL (2021) Description of a new species of *Foenatopus* Smith (Hymenoptera, Stephanidae), with a key to the species from Vietnam. *Journal of Hymenoptera Research* 88: 71–83. <https://doi.org/10.3897/jhr.88.76421>
- Ge SX, Ren LL, Tan JL (2022) First discovery of *Megischus* Brullé (Hymenoptera, Stephanidae) in Ryukyu Islands, with description of a new species. *Journal of Hymenoptera Research* 91: 309–320. <https://doi.org/10.3897/jhr.91.85373>

- Ge SX, Shi HL, Ren LL, Tan JL (2021) Description of a new species of *Megischus* Brullé (Hymenoptera, Stephanidae), with a key to the species from China. *ZooKeys* 1022: 65–77. <https://doi.org/10.3897/zookeys.1022.62833>
- Goloboff PA, Farris JS, Nixon KC (2008) TNT, a free program for phylogenetic analysis. *Cladistics* 24: 774–786.
- Haliday AH (1839) Hymenopterorum Synopsis ad methodum clm. Falleni ut plurimum accomodata, 4 pp. In: Haliday, A.H. Hymenoptera Britannica. London, Hippolytus Ballière (Fasc. 1 and 2), 16 and 28 and 4 pp.
- Hong CD, van Achterberg C, Xu ZF (2010) A new species of *Megischus* Brullé (Hymenoptera, Stephanidae) from China, with a key to the Chinese species. *ZooKeys* 69: 59–64. <https://doi.org/10.3897/zookeys.69.738>
- Hong CD, van Achterberg C, Xu ZF (2011) A revision of the Chinese Stephanidae (Hymenoptera, Stephanoidea). *ZooKeys* 110: 1–108. <https://doi.org/10.3897/zookeys.110.918>
- Huelsenbeck JP, Ronquist F (2001) MRBAYES: Bayesian inference of phylogeny. *Bioinformatics* 17: 754–755. <https://doi.org/10.1093/bioinformatics/17.8.754>
- Jouault C, Rasnitsyn AP, Perrichot V (2021) Ohlhoffiidae, a new Cretaceous family of basal parasitic wasps (Hymenoptera: Stephanoidea). *Cretaceous Research* 117: 104635. <https://doi.org/10.1016/j.cretres.2020.104635>
- Jurine L (1807) Nouvelle Méthode de classer les Hyménoptères et les Diptères. Hyménoptères. Genève, J. J. Paschoud ed. Tome premier. (1)–(4)+1–319, tab. i–xiv.
- Kirk AA (1975) Siricid woodwasps and their associated parasitoids in the south-western United States (Hymenoptera: Siricidae). *The Pan-Pacific Entomologist* 51: 57–61.
- Königsmann E (1978) Das phylogenetische System der Hymenoptera, Teil 4: Aculeata (Unterordnung Apocrita). *Deutsche Entomologische Zeitschrift* 25: 365–435. <https://doi.org/10.1002/mmnd.19780250408>
- Leach WE (1815) Entomology. In: Brewster, D. The Edinburgh Encyclopedia. Vol. 9:2 + 766 pp. Edinburgh. [Publication year not provided on the original publication].
- Legg DA, Sutton MD, Edgecombe GD (2013) Arthropod fossil data increase congruence of morphological and molecular phylogenies. *Nature Communications* 4: 2485. <https://doi.org/10.1038/ncomms3485>
- Lepage T, Bryant D, Philippe H, Lartillot N (2007) A general comparison of relaxed molecular clock models. *Molecular Biology and Evolution* 24(12): 2669–2680
- Lewis PO (2001) A likelihood approach to estimating phylogeny from discrete morphological character data. *Systematic Biology* 50: 913–925. <https://doi.org/10.1080/106351501753462876>
- Li LF, Shih C, Ren D (2013) Two new wasps (Hymenoptera: Stephanoidea: Ephialtitidae) from the Middle Jurassic of China. *Acta Geologica Sinica* 87(6): 1486–1494.
- Li LF, Shih C, Rasnitsyn AP, Ren D (2015) New fossil ephialtitids elucidating the origin and transformation of the propodeal-metasomal articulation in Apocrita (Hymenoptera). *BMC Evolutionary Biology* 15(1): 317. <https://doi.org/10.1186/s12862-015-0317-1>
- Li LF, Rasnitsyn AP, Labandeira CC, Shih C, Ren D (2017) Phylogeny of Stephanidae (Hymenoptera: Apocrita) with a new genus from Upper Cretaceous Myanmar amber. *Systematic Entomology* 42: 194–203. <https://doi.org/10.1111/syen.12202>
- Maddison WP, Maddison DR (2011) Mesquite: A Modular System for Evolutionary Analysis. Version 2.75. URL <http://mesquiteproject.org> [accessed on May 2022].
- Nixon KC (2002) WinClada. Published by the author, Ithaca, New York.
- Peters RS, Krogmann L, Mayer C, Donath A, Gunkel S, Meusemann K, Kozlov A, Podsiadlowksi L, Petersen M, Lanfear R, Diez PA, Heraty J, Kjer KM, Klopstein S, Meier R, Polidori C, Schmitt T, Liu S, Zhou X, Wappler T, Rust J, Misof B, Niehuis O (2017) Evolutionary history of the Hymenoptera. *Current Biology* 27: 1013–1018. <https://doi.org/10.1016/j.cub.2017.01.027>
- Rasnitsyn AP, Zhang HC (2010) Early evolution of Apocrita (Insecta, Hymenoptera) as indicated by new findings in the Middle Jurassic of Daohugou, Northeast China. *Acta Geologica Sinica (English Edition)* 84: 834–873.
- Rasnitsyn AP (1969) [Origin and evolution of the lower Hymenoptera] Trudy Paleontologicheskogo Instituta. Akademiya Nauk SSSR 123, pp. 1–195. (In Russian). English translation, 1979. United States Department of Agriculture, Washington, D.C.
- Ronquist F, Huelsenbeck JP (2003) MrBayes 3: Bayesian phylogenetic inference under mixed models. *Bioinformatics* 19: 1572–1574. <https://doi.org/10.1093/bioinformatics/btg180>
- Ronquist F, Teslenko M, van der Mark P, Ayres DL, Darling A, Höhna S, Larget B, Liu L, Suchard MA, Huelsenbeck JP (2012) MRBAYES 3.2: Efficient Bayesian phylogenetic inference and model selection across a large model space. *Systematic Biology* 61: 539–542. <https://doi.org/10.1093/sysbio/sys029>
- Santos BF, Payne A, Pickett KM, Carpenter JM (2015) Phylogeny and historical biogeography of the paper wasp genus *Polistes* (Hymenoptera: Vespidae): implications for the overwintering hypothesis of social evolution. *Cladistics* 31: 535–549. <https://doi.org/10.1111/cla.12103>
- Sharkey MJ, Carpenter JM, Vilhelmsen L, Heraty J, Liljeblad J, Dowling AP, Schulmeister S, Murray D, Deans AR, Ronquist F, Krogmann L, Wheeler WC (2012) Phylogenetic relationships among superfamilies of Hymenoptera. *Cladistics* 28: 80–112. <https://doi.org/10.1111/j.1096-0031.2011.00366.x>
- Shih C, Li LF, Ren D (2017) Application of geometric morphometric analyses to confirm two new species of Karatavitoidea (Hymenoptera: Karatavitoidea) from northeastern China. *Alcheringa* 41: 499–508. <https://doi.org/10.1080/03115518.2017.1316872>
- Simões TR, Caldwell MW, Palci A, Nydam RL (2017) Giant taxon-character matrices: quality of character constructions remains critical regardless of size. *Cladistics* 33: 198–219. <https://doi.org/10.1111/cla.12163>
- Tan JL, Fan XL, van Achterberg C, Li T (2015a) A new species of *Pseudomegischus* van Achterberg from China, with a key to the species (Hymenoptera, Stephanidae). *ZooKeys* 537: 103–110. <https://doi.org/10.3897/zookeys.537.6592>
- Tan JL, van Achterberg C, Tan QQ, Zhou T, Li T (2018) *Parastephanellus* Enderlein (Hymenoptera: Stephanidae) revisited, with description of two new species from China. *Zootaxa* 4459(2): 327–349. <https://doi.org/10.11646/zootaxa.4459.2.7>
- Tan QQ, van Achterberg C, Tan JL, Chen XX (2015b) A new species of *Schlettererius* Ashmead from China, with a key to the species (Hymenoptera, Stephanidae). *Journal of Hymenoptera Research* 45: 75–86. <https://doi.org/10.3897/JHR.45.5069>
- Taylor KL (1967) Parasitism of *Sirex noctilio* F. by *Schlettererius cinctipes* (Cresson) (Hymenoptera: Stephanidae). *Journal of the Australian Entomological Society* 6: 13–19.

- van Achterberg C (2002) A revision of the Old World species of *Megischus* Brullé, *Stephanus* Jurine and *Pseudomegischus* gen. nov., with a key to the genera of the family Stephanidae (Hymenoptera: Stephanidae). *Zoologische Verhandlungen Leiden* 339: 1–206.
- Vilhelmsen L (1997) The phylogeny of lower Hymenoptera (Insecta), with a summary of the early evolutionary history of the order. *Journal of Zoological Systematics Evolutionary Research* 35: 49–70.
- Vilhelmsen L, Turrisi GF, Beutel RG (2008) Distal leg morphology, subgenital organs and host detection in Stephanidae (Insecta, Hymenoptera). *Journal of Natural History* 42(23–24): 1649–1663.
- Zhang C, Wang M (2019) Bayesian tip dating reveals heterogeneous morphological clocks in Mesozoic birds. *Royal Society Open Science* 6(7): 182062. <https://doi.org/10.1098/rsos.182062>
- Zschach JJ (1788) *Museum N. G. Leskeanum. Regnum animale. Pars entomologica. Ad systema entomologiae. Fabricii ordinata.* Lipsiae. Müller. Vol. 1, 136 pp. Tab. Synistrata, fig. 193.

Supplementary Material 1

Table S1

Authors: Ge SX, Jiang ZH, Ren LL, van Achterberg C, Tan JL (2023)

Data type: .xlsx

Explanation note: List of investigated taxa and related information in the phylogenetic analyses.

Copyright notice: This dataset is made available under the Open Database License (<http://opendatacommons.org/licenses/odbl/1.0>). The Open Database License (ODbL) is a license agreement intended to allow users to freely share, modify, and use this Dataset while maintaining this same freedom for others, provided that the original source and author(s) are credited.

Link: <https://doi.org/10.3897/asp.81.e107579.suppl1>

Supplementary Material 2

Figure S1

Authors: Ge SX, Jiang ZH, Ren LL, van Achterberg C, Tan JL (2023)

Data type: .tif

Explanation note: Strict consensus tree obtained under equal weighting (EW). Solid bullets (●) indicate nonhomoplastic synapomorphies; open bullets (○) indicate homoplastic characters;. Bootstrap value (BS, shown as ‘–’ if absent) and Bremer support values (BR, shown as ‘*’ if absent) are separated by a slash ‘/’ and marked beside of each node.

Copyright notice: This dataset is made available under the Open Database License (<http://opendatacommons.org/licenses/odbl/1.0>). The Open Database License (ODbL) is a license agreement intended to allow users to freely share, modify, and use this Dataset while maintaining this same freedom for others, provided that the original source and author(s) are credited.

Link: <https://doi.org/10.3897/asp.81.e107579.suppl2>

Supplementary Material 3

File S1

Authors: Ge SX, Jiang ZH, Ren LL, van Achterberg C, Tan JL (2023)

Data type: .tif

Explanation note: Nexus file containing the morphological data matrix of 64 characters scored for 61 taxa.

Copyright notice: This dataset is made available under the Open Database License (<http://opendatacommons.org/licenses/odbl/1.0>). The Open Database License (ODbL) is a license agreement intended to allow users to freely share, modify, and use this Dataset while maintaining this same freedom for others, provided that the original source and author(s) are credited.

Link: <https://doi.org/10.3897/asp.81.e107579.suppl3>